A Discrete-Time Model for Daily S&P500 Returns and Realized Variations: Jumps and Leverage Effects *

Tim Bollerslev†
Uta Kretschmer‡
Christian Pigorsch§
George Tauchen¶

First version: March 29, 2005
This version: August 2, 2005

Abstract

We develop an empirically highly accurate discrete-time daily stochastic volatility model that explicitly distinguishes between the jump and continuous-time components of price movements using nonparametric realized variation and Bipower variation measures constructed from high-frequency intraday data. The model setup allows us to directly assess the structural inter-dependencies among the shocks to returns and the two different volatility components. The model estimates suggest that the leverage effect, or asymmetry between returns and volatility, works primarily through the continuous volatility component. The excellent fit of the model makes it an ideal candidate for an easy-to-implement auxiliary model in the context of indirect estimation of empirically more realistic continuous-time jump diffusion and Lévy-driven stochastic volatility models, effectively incorporating the relevant information in the high-frequency data.

JEL Classification: C1, C3, C5, G1

Keywords: Stochastic volatility; Realized volatility; Bipower variation; Jumps; Leverage effect; Return distributions; Simultaneous equation model.

*Uta Kretschmer and Christian Pigorsch acknowledge financial support from the German Academic Exchange Service and the German Research Foundation (SFB 386), respectively. We would also like to thank the participants of the Duke financial econometrics lunch group for helpful comments.

†Department of Economics, Duke University, Box 90097, Durham, NC 27708. E-mail: boller@econ.duke.edu. Phone: +1 919 660 1846

‡Department of Economics, University of Bonn, D-53113 Bonn, Adenauerallee 24-42. E-mail: uta.kretschmer@uni-bonn.de. Phone: +49 (0)228 73 9204

§Department of Statistics, University of Munich (LMU), D-80799 München, Akademiestr 1/I. E-mail: pigorsch@stat.uni-muenchen.de. Phone: +49 (0) 89 21 80 - 35 22.

¶Department of Economics, Duke University, Box 90097, Durham, NC 27708. E-mail: george.tauchen@duke.edu. Phone: +1 919-660-1812.

1 Introduction

Modeling of financial market volatility has been one of the most active areas of research in empirical finance and time series econometrics over the past two decades. A current theme in this literature concerns the question of whether financial prices, and equity prices in particular, may be adequately described by continuous sample path processes, or whether the price movements exhibit discontinuities, or jumps.[1]

One strand of the literature has sought to answer the question through the estimation of specific parametric continuous time models. This literature dates back to the early work of Merton (1976), with more recent contributions allowing for both jumps and time-varying stochastic volatility including Andersen et al. (2002), Bates (2000), Chernov et al. (2003), Eraker (2004), Eraker et al. (2003), and Pan (2002), among others. Still, the estimation of parametric jump diffusion models remains difficult, and the existing empirical results based on daily or coarser frequency data typically do not allow for a very clear distinction between pure diffusive multi-factor stochastic volatility models and lower-order models with jumps. Of course, given the often large within-day price movements, the daily data most often used in the estimation of the models may simply not be informative enough to provide a firm answer. At the same time, the direct estimation of specific parametric volatility models with large samples of high-frequency intraday data remains extremely challenging from a computational perspective and moreover requires that all of the market microstructure complications inherent in the high-frequency data be properly incorporated into the model.

This in turn has motivated a second more recent strand of the literature in which the intraday data is used in the construction of lower-frequency nonparametric daily volatility measurements. This literature, beginning with the work of Andersen and Bollerslev (1998), Andersen et al. (2001b), and Barndorff-Nielsen and Shephard (2002b), builds on the general result that under ideal conditions the sum of successively finer sampled high-frequency squared returns converges to the quadratic variation of the price process. The quadratic variation, of course, includes both the continuous sample path variation and the jumps. However, combining the realized variation with the realized Bipower variation measure first introduced by Barndorff-Nielsen and Shephard (2004, 2005), allows for a direct nonparametric decomposition of the total price variation into its two separate components. Utilizing these ideas, Andersen et al. (2004) and Huang and Tauchen (2005) both report non-trivial contributions to the overall daily price variation from the jump component.

The nonparametric volatility measures have also inspired the development of a series of new and simple-to-implement reduced form volatility forecasting models in which the realized volatilities are modeled by standard discrete-time time series procedures, examples of which include Andersen et al. (2003, 2004), Corsi (2004), Corsi et al. (2005), Deo et al. (2005), Koopman et al. (2005) and Martens et al. (2004), among others. By effectively incorporating the high-frequency data into the volatility measurements, these simple discrete-time models generally out-perform existing more complicated parametric volatility models based on the corresponding return observations only. The simplicity of these methods, however, comes at the cost of disregarding information about the different volatility components. With the exception of Andersen et al. (2004), who simply included lagged

[1] In addition to the implications for the direct modeling of the price process pursued in the present paper, the answer to this question also has important implications for risk management and asset pricing, with jumps generally rendering hedging much more difficult to implement.

measures for the jump component into a univariate linear forecasting model for the total realized variation, none of the above listed studies have made use of the decomposition of the total variation into its separate continuous and jump components. Meanwhile, the apparent relevance of jumps along with the distinctly different distributional features of the continuous and jump components, supports the idea of a more structured approach to realized volatility modeling.

This is the main theme of the present paper, in which we develop an empirically highly accurate multivariate discrete-time volatility model for the returns and the realized continuous sample path and jump variation measures. Our joint modeling of the returns and the two volatility components in turn allows us to directly assess the importance of the often documented asymmetric relationship between returns and volatility, and whether the observed leverage effect is caused by a negative correlation of the lagged returns with the current continuous volatility component and/or current jumps.[2] We initially estimate the model equation-by-equation under the implicit assumption that the disturbances are independent across the three equations. However, our univariate estimation results reveal important nonlinear contemporaneous dependencies in the disturbances, and we go on to account for these in a general recursive simultaneous equation system, explicitly allowing for contemporaneous nonlinear inter-dependencies. Despite the general and very flexible structure of the model, full information maximum likelihood estimation remains relatively straightforward. The recursive structure also makes simulations from the model easy to implement, which we use in checking different aspects of our final preferred specification. Our model estimates are based on daily realized volatilities and returns constructed from high-frequency five-minute S&P500 index futures over the 1985 to 2004 sample period. As part of our analysis, we also highlight some of the key distributional features of the corresponding daily Bipower variation and relative jump measures that any satisfactory continuous or discrete-time model will have to explain.[3]

The remainder of the paper is organized as follows. Section 2 provides a short review of the relevant theory and construction of the pertinent volatility measures. Section 3 discusses the data and summary statistics for the empirical measures motivating the specification of our model. The formulation of the three basic model equations for the returns, Bipower variation and relative jump series is detailed in Section 4. The resulting equation-by-equation estimates are presented in Section 5, along with an assessment of the cross-equation dependencies in the disturbances. Section 6 describes the full joint triangular model and corresponding maximum likelihood estimates. Simulations from the model are used in Section 7 to further investigate the adequacy of the fit. Section 8 concludes with a brief summary and some suggestions for future research.

2 Realized Volatility, Bipower Variation and Jumps

We begin by a brief review of the relevant theory underlying the different variation measures used in our modeling approach. A more thorough theoretical treatment can be found in Andersen et al. (2001b), Barndorff-Nielsen and Shephard (2002a) and Protter (1995).

[2]The recent empirical analysis in Bollerslev et al. (2005) also points toward the existence of a contemporaneous leverage effect in the form of cross-correlated high-frequency returns and absolute returns.

[3]Corresponding empirical characteristics for the total realized variation have previously been documented in the literature by, e.g., Andersen et al. (2001b,a), Areal and Taylor (2002), Ebens (1999), Martens (2002), Martens and Zein (2004), and Thomakos and Wang (2003).

2.1 Quadratic Variation

Our analysis builds on the theory of quadratic variation. Let p_t denote the logarithmic price of a financial asset. Assume that p_t follows the continuous-time semimartingale jump diffusion process:

$$p_t = \int_0^t \mu(s)ds + \int_0^t \sigma(s)dW(s) + \sum_{j=1}^{N(t)} \kappa(s_j), \tag{1}$$

where the mean process $\mu(t)$ is continuous and of finite variation, $\sigma(t) > 0$ denotes the càdlàg instantaneous volatility, $W(t)$ is a standard Brownian Motion, and the $N(t)$ process counts the number of jumps occurring with possibly time-varying intensity $\lambda(t)$ and jump size $\kappa(s_j)$. The theory of quadratic variation then permits the derivation of nonparametric volatility measures that allow us to decompose the total price variation into its continuous and jump part. In particular, the quadratic variation process of (1),

$$[p]_t = \text{plim} \sum_{j=0}^{n-1} (p_{\tau_{j+1}} - p_{\tau_j})^2, \tag{2}$$

where $\tau_0 = 0 \leq \tau_1 \leq \ldots \leq \tau_n = t$ denotes a sequence of partitions with $\sup_j \{\tau_{j+1} - \tau_j\} \to 0$ for $n \to \infty$, may be expressed as,

$$[p]_t = \int_0^t \sigma^2(s)ds + \sum_{j=1}^{N(t)} \kappa^2(s_j), \tag{3}$$

that is, the *integrated variance* and the sum of the *squared jumps*. Of course, in the popular pure diffusive case where the $N(t)$ counting process is identically equal to zero, the second term disappears and the quadratic variation is simply equal to the integrated variance.

2.2 Realized Variation

Most of our analysis will be focussed on daily returns and volatilities. Hence, for notational simplicity we normalize the daily time interval to unity, denoting the corresponding daily returns by:

$$r_t = p_t - p_{t-1}, \quad t = 1, \ldots. \tag{4}$$

To formally define our empirical volatility measures, denote the day t, jth within-day return by:

$$r_{t,j} = p_{t-1+\frac{j}{M}} - p_{t-1+\frac{(j-1)}{M}}, \quad j = 1, \ldots, M, \tag{5}$$

where M refers to the sampling frequency. The sum of the corresponding squared intradaily returns:

$$RV_t = \sum_{j=1}^{M} r_{t,j}^2, \tag{6}$$

then affords a natural estimator of the *realized quadratic variation*. Following the recent literature we will interchangeably refer to this quantity as the *realized variance* or the

realized volatility. The idea of measuring the ex-post variation of asset prices by summing over more frequently sampled squared returns dates back at least to Merton (1980), and was also applied by French et al. (1987), Hsieh (1991) and Poterba and Summers (1986), and more recently by Taylor and Xu (1997), inter alia. Meanwhile, the notion of realized variation was first formally related to the theory of quadratic variation within the context of finance and time-varying volatility modeling by Andersen and Bollerslev (1998), Andersen et al. (2001b), Barndorff-Nielsen and Shephard (2002b) and Comte and Renault (1998). In particular, it follows from the theory discussed above that the realized variance will generally converge uniformly in probability to the quadratic variation as the sampling frequency, M, of the underlying returns approaches infinity:

$$RV_t \rightarrow \int_{t-1}^{t} \sigma^2(s)ds + \sum_{j=N(t-1)+1}^{N(t)} \kappa^2(s_j). \tag{7}$$

In other words, the realized variance affords an ex-post measure of the true total price variation, including the discontinuous jump part.

In order to distinguish the continuous variation from the jump component, Barndorff-Nielsen and Shephard (2004) first proposed the so-called *Bipower variation* measure, defined by:

$$BV_t = \frac{\pi}{2} \sum_{j=2}^{M} |r_{t,j}||r_{t,j-1}|. \tag{8}$$

Importantly, for increasingly finely sampled returns the Bipower variation measure becomes immune to jumps and consistently (for increasing values of M) estimates the integrated variance:

$$BV_t \rightarrow \int_{t-1}^{t} \sigma^2(s)ds. \tag{9}$$

Consequently, the difference between the realized variance and the Bipower variation affords a simple nonparametric estimator of the contribution to total price variation coming from the jump component.

Meanwhile, the extensive simulation evidence in Huang and Tauchen (2005) suggests that an empirically more robust measure is provided by the relative jump statistic, $RJ_t = (RV_t - BV_t)RV_t^{-1}$, or the corresponding logarithmic ratio:[4]

$$J_t = \log RV_t - \log BV_t. \tag{10}$$

Hence, in the empirical results reported on here, we will rely on a joint model for BV_t and J_t as a way of capturing the distinct components accounting for the total daily price variation. Note, that the J_t measure is in theory restricted to be non-negative. However, in practice for finite values of M, BV_t may exceed RV_t so that J_t becomes negative. In the approach adopted here, we will simply treat these "measurement errors" as part of the J_t process. Alternatively, building on the asymptotic (for increasing M) distribution theory in Barndorff-Nielsen and Shephard (2004), it would be possible to truncate the J_t process,

[4]The empirical evidence in Huang and Tauchen (2005) for S&P500 Index data also suggests that the relative contribution of jumps to the total price variation based upon the RJ_t measure amounts to roughly 7 percent.

and only associate the values beyond a certain threshold with the jump component. This is the approach adopted in Andersen et al. (2004), who rely on a large critical value for identifying only the most significant jumps entering a reduced form univariate forecasting model for RV_t. In contrast, by jointly modeling the returns, the relative jump measure and the Bipower variation, we avoid the arbitrary choice of any pre-specified significance level affecting the selection of significant jumps.

3 Data and Stylized Facts

The theory discussed in the preceding section underlying the consistency of the BV_t and J_t measures formally hinges on the notion of increasingly finer sampled high-frequency returns. In practice, however, the sampling frequency is invariably limited by the actual quotation, or transaction frequency. Moreover, the observed high-frequency prices are further "contaminated" by a host of market microstructure frictions, such as price discreteness and bid-ask spreads. These effects combine to render the basic assumption of a semimartingale price process invalid at the tick-by-tick level. In response to this, a number of authors, including Andersen et al. (2001a,b, 2004), have advocated the use of coarser sampling frequencies as a simple way to alleviate these contaminating effects, while maintaining most of the relevant information in the high-frequency data. This is also the approach adopted here.[5] Specifically, while our primary data consists of tick-by-tick transaction prices for the S&P500 Index futures contracts traded on the Chicago Mercantile Exchange, ranging from January 1, 1985 to December 31, 2004, we follow Andersen et al. (2004) in computing our daily realized variance and jump measures from five-minute returns constructed using the nearest prices to each five-minute mark for the most actively traded contracts. We also exclude all overnight returns.

The resulting daily series are displayed in Figure 1. All of the series display the widely-documented volatility clustering effect. Also, the variance of the logarithmic realized variance exceeds that of the logarithmic Bipower variation series. Consistent with this, the jump series depicted in the last panel exhibits many, mostly positive, small values. Some of these observations may be attributed to measurement errors, but there are also a number of more extreme observations indicative of genuine large-sized jumps on those particular days.

These visual impressions are confirmed by the summary statistics reported in Table 1. In particular, the mean and variance of the realized volatility both exceed the corresponding statistics for the square-root Bipower variation. It follows also from the table that the unconditional distribution of both volatility measures are highly skewed and leptocurtic. However, the logarithmic transform renders both approximately normal. This approximate log-normality is further supported by the kernel density plots presented in Figure 2. Similar results for the realized volatility from other markets have previously been reported in Andersen et al. (2001a,b) among others. Meanwhile, the descriptive statistics and the corresponding kernel density plots for the relative jump measure, J_t, clearly indicate a

[5]Several recent studies have developed alternative procedures to more effectively make use of all the tick-by-tick data, including the notion of an optimal sampling frequency, various pre-filtering procedures, along with appropriate sub-sampling schemes; see, e.g., Aït-Sahalia et al. (2005a,b), Areal and Taylor (2002), Bandi and Russell (2005), Corsi et al. (2001), Curci and Corsi (2003), Hansen and Lunde (2005), and Oomen (2004).

positively skewed and leptokurtic distribution.[6] The unconditional distribution of the daily returns also show the expected excess kurtosis and negative skewness. At the same time, the distribution of the returns standardized by the realized volatility is surprisingly close to Gaussian, as previously documented by Andersen et al. (2001a).[7]

Turning to the last column in the table, all of the volatility measures exhibit highly significant own serial dependencies, as evidenced by the Ljung-Box test statistics for up to tenth order autocorrelation. Furthermore, the sample autocorrelation functions in Figure 3 for the two logarithmic volatility measures show the characteristic hyperbolic decay with autocorrelation coefficients being significant (compared to the conservative Bartlett 95% confidence bands) up to the 125th order, or roughly half-a-year.[8] In contrast, the relative jump measure exhibit much less autocorrelation, with most of the dependency attributable to the first and the fifth lag, corresponding to jumps that are one day and one week apart, respectively.

In addition to the serial correlation in the individual series, any interactions among the series will also be important in the formulation of a fully satisfactory joint model. In this regard, a number of previous studies have pointed toward a negative correlation between past return shocks and current volatility, so that "bad" news tend to be associated with a larger increase in volatility than "good" news of the same absolute magnitude.[9] A common approach for empirically visualizing this asymmetric relationship is provided by the news-impact curve originally suggested by Engle and Ng (1993), and previously used in the realized volatility context by Andersen et al. (2001a). The corresponding plots for the logarithmic realized variance and Bipower variation in Figure 4 both exhibit the expected slight asymmetric response to past standardized returns. Interestingly, however, the jumps seem to be almost unaffected by the past return shocks, and if anything they respond *negatively* to the standardized returns. This also explains, why the asymmetric effect is more pronounced for the pure continuous volatility BV_t component in the second panel, in comparison to the total realized variation RV_t depicted in the first panel.

We next present our discrete-time model designed to account for these different distributional features in the daily return, Bipower variation, and relative jump series.

[6]Note that the sign of the skewness is determined by the specific definition of our jump measure as the ratio of RV_t divided by BV_t. Barndorff-Nielsen and Shephard (2004) in contrast consider the inverse ratio resulting in a negatively skewed distribution.

[7]In the absence of jumps and independence between the innovation processes driving the returns and the volatility, the standardized returns defined by the stylized model in equation (1) should be normally distributed.

[8]This long-memory pattern in equity return volatility has, of course, been observed by many earlier studies in the ARCH and stochastic volatility literature, and several different parametric models based on the notion of fractional integration have been proposed to best account for these dependencies.

[9]Although this phenomenon could be explained through financial leverage, the magnitude for equity index returns is typically too large, and alternative explanations based on a time-varying volatility risk-premium have been pursued by Bekaert and Wu (2000), Campbell and Hentschel (1992), Tauchen (2005), among others. However, the causal directions of the leverage and volatility feedback effects are fundamentally different, and the recent high-frequency data analysis in Bollerslev et al. (2005) point toward a "leverage" type causality. We will return to this issue below.

4 Model

A burgeon literature dating back to Bollerslev (1987) and French et al. (1987) has been concerned with the modeling of daily speculative returns using GARCH and related stochastic volatility models; see, e.g., the review in Bollerlsev et al. (1994). More recently, several studies, including Andersen et al. (2003), Martens et al. (2004), Martens and Zein (2004), Pong et al. (2004), and Thomakos and Wang (2003) among others, have advocated the use of ARFIMA type models, along with approximate long-memory component type structures in Andersen et al. (2004) and Corsi (2004), for modeling the dynamic dependencies in realized volatilities. To the best of our knowledge nobody has yet applied these same ideas to the Bipower variation, nor the relative jump measure considered here.[10] More importantly, we are not aware of any attempts at jointly modeling the daily r_t, BV_t and J_t series within a coherent multivariate framework. We begin our discussion by considering the specification for the integrated volatility process as measured by daily Bipower variation, followed by a discussion of our models for the relative jump component and the daily returns, respectively.

4.1 The Bipower Variation Equation

The realized variation only differs from the Bipower variation (by more than measurement errors) in the presence of jumps. Hence, guided by the recent empirical literature pertaining to the modeling of RV_t cited above, we will here rely on the Heterogenous Autoregressive, or HAR-RV, type model, originally proposed by Corsi (2004) and successfully employed in a closely related context by Andersen et al. (2004), for describing the dynamic dependencies in the BV_t series.[11] However, in contrast to the HAR-RV model estimates reported in Corsi (2004) and Andersen et al. (2004), which are based on simple least squares, we shall here rely on more efficient maximum likelihood estimation techniques explicitly accounting for the time-dependent conditional heteroskedasticity in the residuals from the BV_t model through a separate GARCH type specification for the volatility-of-volatility. A similar estimation approach has also recently been implemented by Corsi et al. (2005).

More specifically, to set up the model we define the logarithmic multiperiod Bipower variation measures by the sum of the corresponding daily logarithmic measures:

$$(\log BV)_{t+1-k:t} = \frac{1}{k}\sum_{j=1}^{k} \log BV_{t-j}, \tag{11}$$

where $k = 5$ and $k = 22$ correspond to (approximately) one week and one month, respec-

[10] In a related context, Andersen et al. (2005) have recently explored the use of ACD type models for characterizing the times between significant, according to the ratio statistic in Huang and Tauchen (2005), jumps.

[11] The HAR model may be seen as an extension of the heterogenous ARCH model first suggested by Müller et al. (1997).

tively.[12] Our HAR-GARCH-BV model then takes the form:

$$\begin{aligned}\log BV_t &= \alpha_0 + \alpha_d \log BV_{t-1} + \alpha_w (\log BV)_{t-5:t-1} + \alpha_m (\log BV)_{t-22:t-1} \\ &\quad + \theta_1 \frac{|r_{t-1}|}{\sqrt{RV_{t-1}}} + \theta_2 I[r_{t-1}<0] + \theta_3 \frac{|r_{t-1}|}{\sqrt{RV_{t-1}}} I[r_{t-1}<0] + \sqrt{h_t} u_t \qquad (12) \\ h_t &= \omega + \sum_{j=1}^{q} \alpha_j (\log BV_{t-1} - x'_{BV}\beta_{BV})^2 + \sum_{j=1}^{p} \beta_j h_{t-j} + \sum_{j=1}^{s} \lambda_j BV_{t-j}. \qquad (13)\end{aligned}$$

The lagged daily, weekly and monthly realized variation measures on the right-hand-side of the $\log BV_t$ equation could, of course, be augmented with additional terms to account for the possibility of even longer-run dependencies. However, the combination of relatively few volatility components often provide a remarkably close approximation to true long-memory dependencies. The remaining, new vis-a-vis the original HAR-RV model in Corsi (2004), terms explicitly allow for a leverage effect in the volatility through the inclusion of the lagged signed returns. The model also permits a level effect in the GARCH model for the volatility-of-volatility. Lastly, to account for deviations from conditional normality, we allow the errors to follow a normal-mixture distribution:

$$u_t \overset{iid}{\sim} \begin{cases} \mathbb{N}_1(0,1) & \text{with probability } (1-p_{u,2}) \\ \mathbb{N}_2(\mu_{u,2}, \sigma^2_{u,2}) & \text{with probability } p_{u,2} \end{cases}. \qquad (14)$$

Having defined the model for the continuous volatility component, we next turn our attention to the specification of the jump component.

4.2 The Jump Equation

Consistent with the results in Andersen et al. (2004) pertaining to the time series of significant squared jumps, the descriptive statistics in Section 3 point toward fairly weak, albeit not zero, own serial dependencies in the relative jump series. To best accommodate this we specify a standard autoregressive model augmented with the same leverage type terms used in the BV_t equation:

$$\begin{aligned}\log\left(\frac{RV_t}{BV_t}\right) &= \delta_0 + \psi_1 \frac{|r_{t-1}|}{\sqrt{RV_{t-1}}} + \psi_2 I[r_{t-1}<0] + \psi_3 \frac{|r_{t-1}|}{\sqrt{RV_{t-1}}} I[r_{t-1}<0] \\ &\quad + \sum_{j=1}^{n} \delta_j \log\left(\frac{RV_{t-j}}{BV_{t-j}}\right) + \nu_t. \qquad (15)\end{aligned}$$

This in turn allows us to disentangle whether the well-documented asymmetric negative relationship between total volatility and return innovations is primarily driven by the response of the continuous volatility component and/or the reaction of the jump component.

Experimentation suggests that the innovations in the jump equation are well described by a mixture of a zero mean Normal Inverse Gaussian (NIG) distribution and an Inverse Gaussian (IG) distribution:

$$\nu_t \overset{iid}{\sim} \begin{cases} \mathbb{NIG}_0(\alpha_{NIG}, \beta_{NIG}, \delta_{NIG}) & \text{with probability } (1-p_{\nu,2}) \\ \mathbb{IG}(\lambda_{IG}, \mu_{IG}) & \text{with probability } p_{\nu,2} \end{cases}. \qquad (16)$$

[12] We follow Corsi (2004) in defining the multi-period logarithmic volatility by the sum of the corresponding one-period logarithmic measures. Almost identical empirical results obtain by using the logarithm of the multi-period realized variances in place of the sum of the logarithms.

Other asymmetric distributions could, of course, be considered, but a mixture based on one distribution having support on the whole real line and the other being defined only on the positive domain appears a natural choice for characterizing the jump innovation distribution. Intuitively, the NIG distribution may be seen as primarily accounting for the small day-to-day fluctuations in the logarithmic realized variance around the logarithmic Bipower variation attributable to measurement errors and small jumps, while the positive IG distribution captures the innovations associated with large genuine jumps, or the right tail of the distribution. Moreover, the NIG and IG distributions both have very flexible shapes, and the superior fit afforded by this particular mixture of distributions is indeed confirmed by our model estimates discussed below.

4.3 The Return Equation

Our final model for the distribution of the daily returns rely on the nonparametric RV_t measure for capturing the total price variability. This same idea has previously been used in the context of modeling daily returns by Forsberg and Bollerslev (2002). Note that even though we do not directly model RV_t, the conditional distribution of the total price variation is readily inferred from our models for the logarithmic Bipower variation and the jumps discussed above based upon the definition in equation (10); i.e., $RV_t \equiv \exp(J_t + \log BV_t)$.

Specifically, allowing for up to d'th order serial correlation, we postulate the following simple autoregressive model for the daily return process:

$$r_t = \gamma_0 + \sum_{j=1}^{d} \gamma_j r_{t-j} + \sqrt{RV_t}\epsilon_t. \tag{17}$$

Our final preferred model takes the innovations to be standard normally distributed:

$$\epsilon_t \overset{iid}{\sim} \mathbb{N}(0,1), \tag{18}$$

but as discussed further below, we also experimented with other more flexible mixtures-of-distributions to allow for deviations from conditional normality. However, broadly consistent with the summary statistics in Table 1, we found that the standard normal distribution provided as good a fit as any of these other distributions.

We next turn to a discussion of the univariate estimation results for this very simple return generating process along with the other two equations for the realized variation measures making up our complete system.

5 Equation–by–Equation Estimation

The triangular structure of the three equation system defined in the preceding sections, means that as long as the disturbances are independent across equations, each of the three models may be estimated efficiently in isolation using standard maximum-likelihood methods. The validity of the assumption of independent disturbances is, of course, questionable, and we will subsequently investigate the adequacy of this based upon the single equation estimates.

The estimation results for each of the three equations, along with the corresponding asymptotic standard errors for the parameter estimates, are reported in Table 2. Figures 5 to 7 show the resulting residuals, their autocorrelation and partial autocorrelation functions, as well as the QQ plots and kernel density estimates. The selection of the autoregressive lags in the different models is based on the Schwarz Bayesian information Criterion (BIC), and all of the lags are kept the same in the subsequent models.

Starting with the results in the first column and the BV_t equation, the estimates directly mirror earlier results in the literature for the HAR-RV realized volatility model. The daily, weekly and monthly volatility components are all highly statistically significant, while the inclusion of the logarithmic Bipower variation measures over biweekly and other horizons do not improve the fit according to the BIC criteria. A standard GARCH(1,1) model without any level effects emerges as the preferred specification for the conditional variance. The estimated GARCH parameters easily satisfy the corresponding stationarity condition $\alpha_1\sigma_u^2 + \beta_1 < 1$, where $\sigma_u^2 = 1 + p_{u,2}\left(\sigma_{u,2}^2 - 1\right)$. The importance of allowing for time-varying volatility is further underscored by the plot of the GARCH conditional standard deviation in Figure 8. The importance of asymmetry, or leverage effect, in the continuous volatility component is directly manifest by the highly significant estimates for the θ_1 and θ_3 parameters. As expected, the point estimates imply that a lagged negative return shock leads to a much larger increase in the volatility than does a positive shock of the same magnitude. In contrast, the level shift in the volatility equation due to negative news is not significant. This latter result mirrors earlier findings for the realized volatility in Martens et al. (2004). The QQ and kernel density plots in Figure 5 indicate that the mixture of two normal distributions does a very good job of capturing the slight skewness and kurtosis inherent in the innovations from the model. Moreover, the autocorrelation and partial autocorrelation functions for the estimated residuals do not reveal any remaining systematic serial correlation within a monthly horizon.

Turning to the jump equation, the autoregressive parameter estimates associated with the first, or daily, and fifth, or weekly, lags are both significant. Still, the magnitude of both coefficients is very small, thus supporting the aforementioned weak own predictability in the jump series. Interestingly, and in sharp contrast to the results for the continuous volatility component, the parameter estimates for ψ_2 and ψ_3 related to the leverage effect suggest that jumps are not asymmetrically affected by lagged return shocks. In fact, if anything the estimate for ψ_1 points to a symmetric, but dampening impact of news on future jumps. The findings of a negative leverage effect in the diffusive volatility component only, is directly in line with most of the parametric jump diffusion models estimated in the recent literature, in which the leverage effect is typically incorporated by allowing for a negative correlation between the two Brownian motions driving the price and continuous volatility processes; see, e.g., the models in Bates (2000), Eraker et al. (2003) and Pan (2002).[13] Our results on the contemporaneous dependencies in the disturbances, discussed below, further supports this particular specification. The QQ-Plot for the residuals from the J_t equation as well as the kernel density plots in Figure 6 show that the distribution of the jump innovations is well described by the NIG-IG mixture.

[13]In the context of a representative agent general equilibrium model, Tauchen (2005) has also recently shown that a positive leverage effect can occur depending on the magnitude of the intertemporal marginal rate of substitution and the degree of risk aversion. It is possible that by explicitly differentiating between the two sources of risk, an extension of this model could help explain our empirical findings of a "standard" negative leverage effect in the diffusive component but a positive correlation between returns and jumps.

The estimates for the return equation in the last column reveal statistically significant, but economically very small, second and third order autocorrelations. As already noted, the standard normal distribution fit the data very well, and are generally preferred over other specifications by the BIC criteria, including a normal with a freely estimated variance parameter as well as a freely estimated zero-mean NIG distribution. We also experimented with the inclusion of a risk premia, or GARCH-in-Mean type effect, by allowing the conditional mean to depend on the realized variance. However, consistent with existing results in the literature suggesting that reliable estimates for this risk premium parameter requires longer return horizons and time-spans of data (see e.g. Lundblad (2004) and Ghysels et al. (2005)), we found the GARCH-in-Mean effect to be insignificant at the daily level.

5.1 Residual Inter-Dependencies

The separate estimation of the three equations discussed above implicitly assumes that the disturbances are independent. However, based upon existing results in the stochastic volatility literature, we might naturally expect that the disturbances in the return and volatility equations are correlated due to contemporaneous (at the daily level) leverage and/or volatility feedback effects; see, e.g., the recent high-frequency data analysis in Bollerslev et al. (2005). Moreover, the innovations to the two volatility equations might naturally be expected to be correlated as well. Such inter-dependencies would obviously have to be taken into account in a fully efficient estimation of the joint system, and could also result in inconsistent equation-by-equation estimates.

To begin, consider the sample correlation matrix for the estimated residuals from the Bipower variation, jump and return equations, respectively:

$$\hat{\rho} = \begin{bmatrix} 1 & -0.1847 & -0.2008 \\ . & 1 & 0.0283 \\ . & . & 1 \end{bmatrix}.$$

Consistent with the discussion above, the continuous volatility innovations appear to be negatively correlated with both the relative jump residuals and the return innovations. Meanwhile, the correlation between the relative jumps and the return residuals appears negligible.

In addition to the linear contemporaneous relationships suggested by the sample correlations, there might also exist non-linear dependencies due to, e.g., asymmetric volatility effects. To this end, Figures 9-11 present the pairwise scatter plots of the residual series along with a fitted quadratic polynomial, as well as a Rosenblatt-Parzen Gaussian-based kernel estimator. The conjecture of a nonlinear relationship between the residuals is, obviously, supported for at least two of the three combinations. Most obviously, there is an asymmetric negative relation between the residuals of the Bipower equation and the return shocks in Figure 9. In fact, this relationship is very similar to the usually assumed lagged leverage effect. In contrast, there is no apparent non-linear relation between the residuals from the jump and return equations. Interestingly, Figure 11 reveals a smirk-like relation between the innovations to the continuous volatility and jump components.[14]

[14]This effect should, of course, be carefully interpreted in light of the definitions of the underlying variation measures. In particular, a negative shock to the (logarithmic) Bipower variation corresponds to an overestimation of the continuous volatility component, which in turn is associated with a larger jump component. In contrast, a positive shock to the Bipower variation equation, and a larger than expected continuous volatility component, does not directly affect the relative jump measure.

To further visualize the inter-dependencies between the residual series, Figure 12 shows the scatter plot of the respective pairwise cumulative distribution functions (cdf). In the absence of any dependencies the points should be uniformly distributed over the whole scatter surface. However, consistent with the aforementioned smile-like pattern in the residual scatter plot for the Bipower variation and return equations, the first panel shows that low (high) cdf values of the return innovations tend to be associated with higher cdf values of the diffusive volatility innovations. A similar pattern emerge in the cdf scatter for the jump and continuous volatility innovations in the bottom panel, but with high return cdf values being associated with smaller values of the jump innovation cdf due to the dampening (smirk-like) behavior. Meanwhile, the cdf scatter between the jump and return innovations in the middle panel exhibits nearly uniformly distributed scatter points.

In summary, our analysis points to the existence of important asymmetric dependencies among the three innovation series. These effects should be incorporated into a joint modeling framework in order to, firstly, more systematically quantify and test for their significance, secondly, guard against any biases in the single equation estimates, and thirdly, enhance the efficiency of the individual model parameter estimates. The unified system approach explicitly allowing for non-linear functional forms of residual dependencies developed in the next section does this.

6 System Estimation

The results of the equation–by–equation estimations suggest that the proposed model specifications provide an adequate description of the dynamic dependencies in the two volatility and return processes, but that it does not fully account for the nonlinear contemporaneous dependencies among the innovations. We therefore retain our basic three equation set up, but additionally model the nonlinear inter-dependencies based on the following system of equations:

$$
\begin{aligned}
r_t &= \gamma_0 + \sum_{j=1}^{d} \gamma_j r_{t-j} + \sqrt{RV_t}\epsilon_t \\
\log BV_t &= \alpha_0 + \alpha_d \log BV_{t-1} + \alpha_w (\log BV)_{t-5:t-1} + \alpha_m (\log BV)_{t-22:t-1} \\
&\quad + \theta_1 \frac{|r_{t-1}|}{\sqrt{RV_{t-1}}} + \theta_2 I[r_{t-1}<0] + \theta_3 \frac{|r_{t-1}|}{\sqrt{RV_{t-1}}} I[r_{t-1}<0] + \sqrt{h_t}\,(u_t + g(\epsilon_t)) \\
h_t &= \omega + \sum_{j=1}^{q} \alpha_j \left(\log BV_{t-j} - x'_{BV}\beta_{BV}\right)^2 + \sum_{j=1}^{p} \beta_j h_{t-j} + \sum_{j=1}^{s} \lambda_j BV_{t-j} \qquad (19) \\
\log\left(\frac{RV_t}{BV_t}\right) &= \delta_0 + \sum_{j=1}^{n} \delta_j \log\left(\frac{RV_{t-j}}{BV_{t-j}}\right) \\
&\quad + \psi_1 \frac{|r_{t-1}|}{\sqrt{RV_{t-1}}} + \psi_2 I[r_{t-1}<0] + \psi_3 \frac{|r_{t-1}|}{\sqrt{RV_{t-1}}} I[r_{t-1}<0] \\
&\quad + (\nu_t + m(u_t) + k(\epsilon_t))\,.
\end{aligned}
$$

In comparison to the individual equations, the system explicitly allows the innovations in the continuous volatility and relative jump equations to depend nonlinearly on the return innovations via the general functions $g(\epsilon_t)$ and $k(\epsilon_t)$, respectively. Similarly, the

jump innovations are allowed to depend on the continuous volatility shocks via the $m(u_t)$ function. Thus, by choosing an adequate functional form for each of these functions, we seek to render the underlying three innovation series to be pairwise independent.

Now, utilizing the triangular structure of the basic model equations along with the contemporaneous independence of the transformed innovations, the transition density for the joint system, $y_t = (\log BV_t, \log\left(\frac{RV_t}{BV_t}\right), r_t)'$, may be readily expressed as:

$$
\begin{aligned}
f_y(y_t|x_{t-1};\theta) &= \frac{1}{\sqrt{h_t}\sqrt{RV_t}} \\
&\times f_\epsilon\left(\underbrace{\frac{r_t - x_r'\beta_r}{\sqrt{RV_t}}}_{\epsilon_t}\middle|\vartheta_\epsilon\right) f_u\left(\underbrace{\frac{\log BV_t - x_{BV}'\beta_{BV}}{\sqrt{h_t}} - g\left(\frac{r_t - x_r'\beta_r}{\exp\left\{\frac{1}{2}\log RV_t\right\}}\right)}_{u_t}\middle|\vartheta_u\right) \\
&\times f_\nu\left(\underbrace{\log\left(\frac{RV_t}{BV_t}\right) - x_{RV}'\beta_{RV} - m(u_t) - k(\epsilon_t)}_{\nu_t}\middle|\vartheta_\nu\right),
\end{aligned}
$$

where as before:

$$
\begin{aligned}
\epsilon_t &\overset{iid}{\sim} \mathbb{N}(0,1) \\
u_t &\overset{iid}{\sim} \begin{cases} \mathbb{N}_1(0,1) & \text{with probability } (1-p_{u,2}) \\ \mathbb{N}_2(\mu_{u,2}, \sigma_{u,2}^2) & \text{with probability } p_{u,2} \end{cases} \\
\nu_t &\overset{iid}{\sim} \begin{cases} \mathbb{NIG}_0(\alpha_{NIG}, \beta_{NIG}, \delta_{NIG}) & \text{with probability } (1-p_{\nu,2}) \\ \mathbb{IG}(\lambda_{IG}, \mu_{IG}) & \text{with probability } p_{\nu,2}. \end{cases}
\end{aligned}
$$

To complete the specification, we assume that the nonlinear contemporaneous dependencies among the individual equation innovations may be adequately captured by a set of second order degree polynomials:[15]

$$g(\epsilon_t) = g_1\epsilon_t + g_2\epsilon_t^2 \tag{20}$$

$$k(\epsilon_t) = k_1\epsilon_t + k_2\epsilon_t^2 \tag{21}$$

$$m(u_t) = m_1 u_t + m_2 u_t^2, \tag{22}$$

where for identification purposes we have restricted the three constants to be zero. Fully efficient maximum likelihood estimation of the complete system may now proceed in a standard manner by maximizing the log likelihood function defined by the summation of the logarithmic transition densities over the sample observations.

[15] We also experimented with higher order polynomials, but found a simple quadratic sufficient in capturing the smirk-like dependencies over the required range.

Comparing the system estimation results reported in Table 3 to the equation-by-equation results in Table 2, the estimates for most of the individual parameters obviously do not change by much. In particular, our previous conclusions regarding the lagged leverage effect in the continuous volatility component and the positive correlation between jump and return innovations all remain intact.[16] Moreover, as expected the asymptotic standard errors for the estimated parameters are generally smaller for the system estimates in Table 3, highlighting the gain in (asymptotic) efficiency obtained by jointly estimating the three equations.

Along these lines, the highly significant quadratic term in the $g(\epsilon_t)$ dependency function clearly indicates that the innovations to the continuous volatility component are nonlinearly related to the innovations to the return equation. In contrast, for the return and jump innovations only k_1 is significant and both of the parameters are numerically very small. The aforementioned non-linear relationship between the continuous volatility component and the relative jump innovations allowed for by the $m(u_t)$ dependency function is also strongly supported by the joint estimation. The importance of allowing for contemporaneous nonlinear dependencies among the innovations is further underscored by the Likelihood-Ratio test comparing the fully specified simultaneous equation model to the system equation estimates without the quadratic polynomials, which equals an overwhelmingly significant 597.67.

The model presented in Table 3 still includes some individually insignificant parameters. In particular, restricting $\theta_2 = \psi_2 = \psi_3 = k_2 = 0$, and re-estimating the model results in a LR test statistic of only 6.619 versus the fully general model. Also, the remaining parameter estimates are hardly affected by restricting these four parameters to be equal to zero. Our final preferred model specification is therefore given by this restricted model in Table 4.

As an additional diagnostic check for this final specification, consider the sample correlation between the three residual series:

$$\hat{\rho} = \begin{bmatrix} 1 & -0.0221 & -0.0096 \\ . & 1 & -0.0046 \\ . & . & 1 \end{bmatrix}.$$

Compared to the sample correlations for the equation-by-equation residuals reported earlier, these are obviously much closer to zero and generally insignificant. The three scatter plots for the pairwise cdf's for the system residuals in Figure 13 now also appear uniformly distributed over the entire range, indicating that the quadratic polynomials have successfully accounted for the nonlinear contemporaneous dependencies observed in the equation-by-equation residuals.

7 Model Simulations

The discussion in the previous section suggests that the model performs an exemplary job in terms of describing the one-day-ahead conditional transition densities when judged by the standard maximum likelihood criteria and corresponding model diagnostics.[17] Meanwhile,

[16] Importantly, the system GARCH parameter estimates for the BV_t equations also satisfy the corresponding second-order stationarity condition: $\alpha\left(\sigma_u^2 + g_1^2 + 2g_2^2\right) + \beta < 1$, where $\sigma_u^2 = 1 + p_{u,2}\left(\sigma_{u,2}^2 - 1\right)$ and $\alpha \geq 0$, $\beta \geq 0$.

[17] Although not reported in the paper, we have also investigated the dynamic patterns and distributional assumptions of the system residuals yielding almost identical results to the ones for the single-equation

in order to better understand the workings and possible limitations of a given model, it is often instructive to consider its ability to account for other aspects of the data through the use of simulations. To this end, we generate 105,040 observations from the estimated system, keeping only the last 5,040 observations corresponding to the sample size of our data; i.e., the first 100,000 simulated observations serve as a large burn-in period. We then repeat this 25,000 times, leaving us with 25,000 simulated "daily" sample paths for the returns, logarithmic Bipower variation, and relative jump series. To illustrate, Figure 14 shows one such representative set of simulated data. The basic similarities for each of the series with those of the original data in Figure 1 are striking, and indeed shows the model to be broadly consistent with the data.

More formally, consider the summary statistics in Table 1. By calculating the same set of summary statistics for each of the 25,000 simulated sample paths, we obtain a model-implied sample distribution for the respective statistics. If the model provides an adequate description of the observed data, the realized values of the corresponding sample statistics should lie within reasonable confidence intervals, say 95%, of these model-implied distributions. Table 5 provides these 95% simulated confidence intervals for the standard set of summary statistics, as well as the actual sample values from Table 1. We also report actual and simulated quantiles for each of the series, and illustrate these in Figure 15. Nearly all of the sample statistics, including all of the reported 0.01 to 0.99 quantiles, lie within the simulated confidence bands. Only the realized skewness and kurtosis for the returns and the realized kurtosis for the logarithmic Bipower variation fall outside the 95% bands.[18]

Exploring the dynamic implications of the model, Figure 16 shows the sample autocorrelations and partial autocorrelations with the corresponding simulated 95% confidence bands. As can be seen from the figure, the short-run dynamics of both the returns and the relative jump series are generally consistent with those of the model. Meanwhile, the HAR model for $\log BV_t$, as well as the model's implications for $\log RV_t$, both fall somewhat short in terms of reproducing the highly significant and very slowly decaying sample autocorrelations over longer multi-month lags.[19] At the same time, however, Figure 17 shows that the autocorrelations for the Bipower and realized variation expressed in standard deviation form, as would be of interest in many practical applications, both are well accounted for by our relatively simple and easy-to-implement final preferred model in Table 4.

8 Conclusion

Motivated by the recent empirical results on the relevance of jumps to total price variation derived from high-frequency based realized volatility and Bipower variation measures, this paper develops a joint discrete-time model for returns and volatility, explicitly disentan-

estimates in Figures 5 to 7. These results are available upon request.

[18] Although our maximum likelihood based inference doesn't seem to favor this, this could presumable be "fixed" by allowing for a fattailed and skewed error distribution in the return equation, either parametrically or through the uses of more flexible semi-nonparametric density estimation as in, e.g., Gallant and Nychka (1987) and Gallant and Tauchen (1989).

[19] As previously noted, the inclusion of quarterly or longer-run realized variation measures on the right-hand-side of the HAR model for $\log BV_t$ would presumable remedy this deficiency; see also the simulations reported in Corsi (2004), which shows that the HAR model can get remarkably close to reproducing the autocorrelations of a true long-memory volatility process.

gling the dynamics of the continuous volatility and jump components. We show that the often observed leverage effect, or asymmetry in the lagged return volatility relationship, primarily acts through the continuous volatility component. Our joint modeling approach also facilitates a closer examination of the inter-dependencies among the different shocks, in turn revealing a similar contemporaneous asymmetry among the innovations. Our findings are thus in line with most of the parametric continuous time jump diffusion models employed in the literature, which typically introduce the leverage effect by correlating the Brownian motions driving the return and continuous volatility processes. The discrete-time modeling strategy followed here has several advantages over some of the other reduced-form realized volatility and GARCH modeling procedures recently considered in the literature.

First, consistent with the exploratory analysis in Andersen et al. (2004), by explicitly disentangling the dynamics of the two volatility components, our results clearly show that the jumps are much less persistent, and hence less predictable, than the continuous sample path variation. This in turn should result in improved volatility forecasts, with direct and important implications for interval forecasts and corresponding risk management decisions. If the two volatility components carry different risk premia, it also becomes of the utmost importance for the pricing of options and other derivative instruments to separately model and forecast each of the components.

Second, by providing a highly accurate description of the discrete-time joint dynamics of the returns and the two volatility components, our model can be used in the indirect estimation of other parametric volatility models, effectively incorporating the relevant information contained in the high-frequency data.[20] More specifically, the flexibility and recursive structure of the model coupled with the ready availability of its analytic derivatives, combine to make it an ideal candidate for the role of auxiliary model, or score generator, within the Efficient Method of Moment (EMM) estimation framework of Gallant and Tauchen (1996). As such, our results hold the promise for the formulation and estimation of much richer and empirically realistic Poisson jump diffusion or more general Lévy-driven continuous time stochastic volatility models. We leave further work along these lines for future research.

[20]High-frequency data based nonparametric realized volatility measures have previously been used in the estimation of parametric continuous time stochastic volatility models by Barndorff-Nielsen and Shephard (2002a) employing a Kalman filtering technique, and Bollerslev and Zhou (2002) using a simple GMM-type estimation procedure.

References

Aït-Sahalia, Y., Mykland, P. A., and Zhang, L. (2005a), "How Often to Sample a Continuous-Time Process in the Presence of Market Microstructure Noise," *Review of Financial Studies*, 18, 351–416.

— (2005b), "A Tale of Two Time Scales: Determining Integrated Volatility with Noisy High-Frequency Data," *Journal of the American Statistical Association*, forthcoming.

Andersen, T., Bollerlsev, T., and Huang, X. (2005), "A Semiparametric Framework for Modeling and Forecasting Jumps and Volatility in Speculative Prices," Tech. rep., Duke University.

Andersen, T. G., Benzoni, L., and Lund, J. (2002), "An Empirical Investigation of Continuous-Time Equity Return Models," *Journal of Finance*, 57, 1239–1284.

Andersen, T. G. and Bollerslev, T. (1998), "Answering the Skeptics: Yes, Standard Volatility Models do Provide Accurate Forecasts," *International Economic Review*, 39, 885–905.

Andersen, T. G., Bollerslev, T., and Diebold, F. X. (2004), "Some Like it Smooth, and Some Like it Rough: Untangling Continuous and Jump Components in Measuring, Modeling, and Forecasting Asset Return Volatility," Tech. rep., University of Pennsylvania.

Andersen, T. G., Bollerslev, T., Diebold, F. X., and Ebens, H. (2001a), "The Distribution of Realized Stock Return Volatility," *Journal of Financial Economics*, 61, 43–76.

Andersen, T. G., Bollerslev, T., Diebold, F. X., and Labys, P. (2001b), "The Distribution of Realized Exchange Rate Volatility," *Journal of the American Statistical Association*, 96, 42–55.

— (2003), "Modeling and Forecasting Realized Volatility," *Econometrica*, 71, 579–625.

Areal, N. M. P. C. and Taylor, S. J. (2002), "The Realized Volatility of FTSE-100 Futures Prices," *Journal of Futures Markets*, 22, 627–648.

Bandi, F. M. and Russell, J. R. (2005), "Microstructure Noise, Realized Volatility, and Optimal Sampling," Tech. rep., University of Chicago.

Barndorff-Nielsen, O. E. and Shephard, N. (2002a), "Econometric Analysis of Realised Volatility and its Use in Estimating Stochastic Volatility Models," *Journal of the Royal Statistical Society, Series B*, 64, 253–280.

— (2002b), "Estimating Quadratic Variation Using Realized Variance," *Journal of Applied Econometrics*, 17, 457–477.

— (2004), "Power and Bipower Variation with Stochastic Volatility and Jumps," *Journal of Financial Econometrics*, 2, 1–37.

— (2005), "How Accurate is the Asymptotic Approximation to the Distribution of Realised Volatility?" in *Identification and Inference for Econometric Models. A Festschrift for Tom Rothenberg*, eds. Andrews, D., Powell, J., Ruud, P., and Stock, J., Cambridge: Cambridge University Press, pp. ??–??

Bates, D. S. (2000), "Post-'87 Crash Fears in the S&P 500 Futures Option Market," *Journal of Econometrics*, 94, 181–238.

Bekaert, G. and Wu, G. (2000), "Asymmetric Volatility and Risk in Equity Markets," *Review of Financial Studies*, 13, 1–42.

Bollerlsev, T., Engle, R., and Nelson, D. (1994), "ARCH Models," in *Handbook of Econometrics*, eds. Engle, R. and McFadden, D., Amsterdam: Elsevier.

Bollerslev, T. (1987), "A Conditionally Heteroskedastic Time Series Model for Speculative Prices and Rates of Return," *Review of Economics and Statistics*, 69, 542–547.

Bollerslev, T., Litvinova, J., and Tauchen, G. (2005), "Volatility Asymmetry in High Frequency Data," Tech. rep., Duke University.

Bollerslev, T. and Zhou, H. (2002), "Estimating Stochastic Volatility Diffusions Using Conditional Moments of Integrated Volatility," *Journal of Econometrics*, 109, 33–65.

Campbell, J. Y. and Hentschel, L. (1992), "No News is Good News: An Asymmetric Model of Changing Volatility in Stock Returns," *Journal of Financial Economics*, 31, 281–331.

Chernov, M., Gallant, A. R., Ghysels, E., and Tauchen, G. (2003), "Alternative Models for Stock Price Dynamics," *Journal of Econometrics*, 116, 225–257.

Comte, F. and Renault, E. (1998), "Long-Memory in Continuous-Time Stochastic Volatility Models," *Mathematical Finance*, 8, 291–323.

Corsi, F. (2004), "A Simple Long Memory Model of Realized Volatility," Tech. rep., University of Southern Switzerland.

Corsi, F., Kretschmer, U., Mittnik, S., and Pigorsch, C. (2005), "The Volatility of Volatility," Tech. rep.

Corsi, F., Zumbach, G., Müller, U. A., and Dacorogna, M. (2001), "Consistent High-Precision Volatility from High-Frequency Data," *Economic Notes*, 30, 183–204.

Curci, G. and Corsi, F. (2003), "A Discrete Sine Transform Approach for Realized Volatility Measurement," Tech. Rep. 44, National Centre Of Competence in Research Financial Valuation and Risk Management.

Deo, R., Hurvich, C., and Lu, Y. (2005), "Forecasting Realized Volatility using a Long-Memory Stochastic Volatility Model: Estimation, Prediction and Seasonal Adjustment," *Journal of Econometrics*, forthcoming.

Ebens, H. (1999), "Realized Stock Volatility," Tech. rep., John Hopkins University.

Engle, R. F. and Ng, V. K. (1993), "Measuring and Testing the Impact of News on Volatility," *Journal of Finance*, 48, 1749–1778.

Eraker, B. (2004), "Do Stock Prices and Volatility Jump? Reconciling Evidence from Spot and Option Prices," *Journal of Finance*, 59, 1367–1403.

Eraker, B., Johannes, M., and Polson, N. (2003), "The Impact of Jumps in Volatility and Returns," *Journal of Finance*, 58, 1269–1300.

Forsberg, L. and Bollerslev, T. (2002), "Bridging the Gap Between the Distribution of Realized (ECU) Volatility and ARCH Modeling (of the Euro): The GARCH-NIG Model," *Journal of Applied Econometrics*, 17, 535–548.

French, K. R., Schwert, G. W., and Stambaugh, R. F. (1987), "Expected Stock Returns and Volatility," *Journal of Financial Economics*, 19, 3–29.

Gallant, A. R. and Nychka, D. W. (1987), "Semi-Nonparametric Maximum Likelihood Estimation," *Econometrica*, 55, 363–390.

Gallant, A. R. and Tauchen, G. (1989), "Seminonparametric Estimation of Conditionally Constrained Heterogeneous Processes: Asset Pricing Applications," *Econometrica*, 57, 1091–1120.

— (1996), "Which Moment to Match?" *Econometric Theory*, 12, 657–681.

Ghysels, E., Santa-Clara, P., and Valkanov, R. (2005), "There is a risk-return trade-off after all," *Journal of Financial Economics*, forthcoming.

Hansen, P. and Lunde, A. (2005), "Realized Variance and Market Microstructure Noise," *Journal of Business & Economic Statistics*, forthcoming.

Hsieh, D. A. (1991), "Chaos and Nonlinear Dynamics: Application to Financial Markets," *Journal of Finance*, 46, 1839–1877.

Huang, X. and Tauchen, G. (2005), "The Relative Contribution of Jumps to Total Price Variance," *Journal of Financial Econometrics*, forthcoming.

Koopman, S. J., Jungbacker, B., and Hol, E. (2005), "Forecasting Daily Variability of the S&P 100 Stock Index Using Historical, Realised and Implied Volatility Measurements," *Journal of Empirical Finance*, 12, 445–475.

Lundblad, C. (2004), "The Risk Return Tradeoff in the Long-Run: 1836-2003," Tech. rep.

Martens, M. (2002), "Measuring and Forecasting S&P 500 Index-Futures Volatility Using High-Frequency Data," *Journal of Futures Markets*, 22, 497–518.

Martens, M., Dijk, D. v., and de Pooter, M. (2004), "Modeling and Forecasting S&P 500 Volatility: Long Memory, Structural Breaks and Nonlinearity," Tech. rep., Erasmus University Rotterdam.

Martens, M. and Zein, J. (2004), "Predicting Financial Volatility: High-Frequency Time-Series Forecasts vis-à-vis Implied Volatility," *Journal of Futures Markets*, 24, 1005–1028.

Merton, R. C. (1976), "Option Pricing When Underlying Stock Returns are Discontinuous," *Journal of Financial Economics*, 3, 125–144.

— (1980), "On Estimating the Expected Return on the Market : An Exploratory Investigation," *Journal of Financial Economics*, 8, 323–361.

Müller, U. A., Dacorogna, M. M., Davé, R. D., Olsen, R. B., Pictet, O. V., and von Weizsäcker, J. E. (1997), "Volatilities of Different Time Resolutions - Analyzing the Dynamics of Market Components," *Journal of Empirical Finance*, 4, 213–239.

Oomen, R. C. (2004), "Modelling Realized Volatility When Returns are Serially Correlated," Tech. Rep. SP II 2004-11, Social Science Research Center, Berlin.

Pan, J. (2002), "The Jump-Risk Premia Implicit in Options: Evidence from an Integrated Time-Series Study," *Journal of Financial Economics*, 63, 3–50.

Pong, S., Shackleton, M. B., Taylor, S. J., and Xu, X. (2004), "Forecasting Currency Volatility: A Comparison of Implied Volatilities and AR(FI)MA Models," *Journal of Banking & Finance*, 28, 2541–2563.

Poterba, J. M. and Summers, L. H. (1986), "The Persistence of Volatility and Stock Market Fluctuations," *The American Economic Review*, 76, 1142–1151.

Protter, P. (1995), *Stochastic Integration and Differential Equations*, vol. 21 of *Applications of Mathematics*, Springer-Verlag, 2nd ed.

Tauchen, G. (2005), "Stochastic Volatility in General Equilibrium," Tech. rep., Duke University.

Taylor, S. J. and Xu, X. (1997), "The Incremental Volatility Information in One Million Foreign Exchange Quotations," *Journal of Empirical Finance*, 4, 317–340.

Thomakos, D. D. and Wang, T. (2003), "Realized Volatility in the Futures Markets," *Journal of Empirical Finance*, 10, 321–353.

Table 1: Descriptive Statistics

Series	Mean	Std.Dev.	Median	Skewness	Exc.Kurt.	Ljung-Box(10)[1]
$\sqrt{RV_t}$	0.8627	0.5935	0.7586	15.3509	496.7651	10155.72
$\log RV_t$	-0.5139	0.8775	-0.5527	0.5950	1.7981	22023.20
$\sqrt{BV_t}$	0.8340	0.5359	0.7348	11.1561	288.4633	12223.28
$\log BV_t$	-0.5817	0.8845	-0.6163	0.5418	1.4807	21715.55
$\log\left(\frac{RV_t}{BV_t}\right)$	0.0678	0.1263	0.0538	1.7766	12.2675	51.44
r_t	0.0254	1.0946	0.0511	-2.1655	96.2483	117.29
$r_t/\sqrt{RV_t}$	0.0866	1.0027	0.0739	0.0503	-0.1497	14.86

Table 2: Single Equation Estimation Results

	BV equation			Jump equation			Return equation	
	Estimate	Std. Error		Estimate	Std. Error		Estimate	Std. Error
α_0	-0.1978	(0.0170)	δ_0	0.0704	(0.0067)	γ_0	0.0858	(0.0098)
α_d	0.2548	(0.0169)	δ_1	0.0347	(0.0089)	γ_2	-0.0254	(0.0139)
α_w	0.4370	(0.0265)	δ_5	0.0516	(0.0116)	γ_3	-0.0351	(0.0133)
α_m	0.2416	(0.0215)	ψ_1	-0.0143	(0.0032)			
θ_1	0.0571	(0.0144)	ψ_2	-0.0026	(0.0050)			
θ_2	0.0384	(0.0217)	ψ_3	0.0014	(0.0049)			
θ_3	0.1247	(0.0218)	$p_{\nu,2}$	0.0072	(0.0329)			
ω	0.0228	(0.0053)	α_{NIG}	71.5659	(52.7253)			
α_1	0.0419	(0.0077)	β_{NIG}	54.0383	(47.7732)			
β_1	0.8048	(0.0378)	δ_{NIG}	0.2637	(0.0367)			
$p_{u,2}$	0.1451	(0.0304)	λ_{IG}	0.5247	(0.3198)			
$\mu_{u,2}$	0.7688	(0.1306)	μ_{IG}	1.1804	(5.2968)			
$\sigma_{u,2}$	1.9278	(0.0688)						
logL:	-3464.75		logL:	3775.22		logL:	-5839.63	

Table 3: System Estimation Results (logL=-5230.37)

	BV equation			Jump equation			Return equation	
	Estimate	Std. Error		Estimate	Std. Error		Estimate	Std. Error
α_0	-0.2526	(0.0172)	δ_0	0.0665	(0.0051)	γ_0	0.0570	(0.0095)
α_d	0.2499	(0.0160)	δ_1	0.0422	(0.0095)	γ_2	-0.0321	(0.0125)
α_w	0.4494	(0.0249)	δ_5	0.0500	(0.0110)	γ_3	-0.0431	(0.0116)
α_m	0.2291	(0.0205)	ψ_1	-0.0145	(0.0033)			
θ_1	0.0636	(0.0139)	ψ_2	-0.0034	(0.0050)			
θ_2	0.0424	(0.0215)	ψ_3	0.0028	(0.0051)			
θ_3	0.1246	(0.0211)	m_1	-0.0200	(0.0012)			
g_1	-0.2493	(0.0186)	m_2	0.0013	(0.0004)			
g_2	0.1363	(0.0129)	k_1	0.0042	(0.0015)			
ω	0.0250	(0.0055)	k_2	0.0018	(0.0011)			
α_1	0.0425	(0.0077)	$p_{\nu,2}$	0.0174	(0.0263)			
β_1	0.7707	(0.0417)	α_{NIG}	41.8149	(13.6452)			
$p_{u,2}$	0.1617	(0.0035)	β_{NIG}	26.1884	(11.2286)			
$\mu_{u,2}$	0.6183	(0.1204)	δ_{NIG}	0.2417	(0.0330)			
$\sigma_{u,2}$	1.9391	(0.0731)	λ_{IG}	0.3183	(0.0933)			
			μ_{IG}	0.3722	(0.7001)			

Table 4: Restricted System Estimation Results (logL=-5233.67)

BV equation			Jump equation			Return equation		
	Estimate	Std. Error		Estimate	Std. Error		Estimate	Std. Error
α_0	-0.2351	(0.0140)	δ_0	0.0668	(0.0042)	γ_0	0.0572	(0.0095)
α_d	0.2510	(0.0160)	δ_1	0.0426	(0.0094)	γ_2	-0.0323	(0.0125)
α_w	0.4476	(0.0249)	δ_5	0.0497	(0.0110)	γ_3	-0.0430	(0.0116)
α_m	0.2298	(0.0205)	ψ_1	-0.0136	(0.0025)			
θ_1	0.0489	(0.0115)	ψ_2	-	-			
θ_2	-	-	ψ_3	-	-			
θ_3	0.1596	(0.0126)	m_1	-0.0200	(0.0012)			
g_1	-0.2493	(0.0186)	m_2	0.0013	(0.0004)			
g_2	0.1406	(0.0127)	k_1	0.0045	(0.0015)			
ω	0.0247	(0.0055)	k_2	-	-			
α_1	0.0419	(0.0077)	$p_{\nu,2}$	0.0198	(0.0236)			
β_1	0.7728	(0.0416)	α_{NIG}	41.0467	(12.6795)			
$p_{u,2}$	0.1628	(0.0355)	β_{NIG}	25.6054	(10.3213)			
$\mu_{u,2}$	0.6149	(0.1194)	δ_{NIG}	0.2390	(0.0322)			
$\sigma_{u,2}$	1.9374	(0.0730)	λ_{IG}	0.3007	(0.0830)			
			μ_{IG}	0.3264	(0.5295)			

Table 5: Simulation

	r_t		$\log RV_t$		$\log BV_t$		$\log\left(\frac{RV_t}{BV_t}\right)$	
stat.	realized	95% intervals	realized	95% intervals	realized	95% intervals	realized	95% intervals
Mean	0.0254	(-0.0125,0.0416)	-0.5139	(-0.7501,-0.3148)	-0.5817	(-0.8159,-0.3788)	0.0678	(0.0611,0.0687)
Std.Dev.	1.0946	(0.8539,1.1504)	0.8775	(0.7382,0.9312)	0.8845	(0.7447,0.9377)	0.1263	(0.1200,0.1354)
Skew.	-2.1648	(-1.8996,0.0906)	0.5948	(-0.0211,0.5765)	0.5416	(-0.0252,0.5711)	1.7761	(0.9838,3.8142)
Exc.Kurt.	96.2483	(3.2207,37.8147)	1.7981	(-0.0476,1.2418)	1.4807	(-0.0354,1.2464)	12.2675	(3.1382,60.7865)
$Q_{0.01}$	-2.6479	(-3.4341,-2.3966)	-2.3275	(-2.7117,-2.0456)	-2.3868	(-2.7956,-2.1305)	-0.1517	(-0.1720,-0.1548)
$Q_{0.025}$	-2.0527	(-2.4330,-1.7798)	-2.0632	(-2.3743,-1.7998)	-2.1377	(-2.4537,-1.8780)	-0.1303	(-0.1394,-0.1268)
$Q_{0.05}$	-1.5535	(-1.7945,-1.3384)	-1.8321	(-2.0994,-1.5834)	-1.9172	(-2.1746,-1.6577)	-0.1027	(-0.1116,-0.1013)
$Q_{0.10}$	-1.0895	(-1.2252,-0.9229)	-1.5848	(-1.7958,-1.3244)	-1.6667	(-1.8696,-1.3969)	-0.0737	(-0.0792,-0.0703)
$Q_{0.25}$	-0.4626	(-0.5275,-0.3872)	-1.1147	(-1.3135,-0.8754)	-1.1859	(-1.3812,-0.9436)	-0.0143	(-0.0225,-0.0147)
$Q_{0.50}$	0.0511	(0.0308,0.0767)	-0.5527	(-0.7797,-0.3452)	-0.6163	(-0.8443,-0.4098)	0.0538	(0.0470,0.0551)
$Q_{0.75}$	0.5446	(0.4790,0.5901)	0.0173	(-0.2421,0.2279)	-0.0533	(-0.3044,0.1683)	0.1339	(0.1264,0.1366)
$Q_{0.90}$	1.0964	(0.9484,1.1850)	0.6022	(0.2553,0.8023)	0.5372	(0.1968,0.7448)	0.2218	(0.2091,0.2242)
$Q_{0.95}$	1.5001	(1.2961,1.6478)	0.9853	(0.5634,1.1937)	0.9352	(0.5084,1.1375)	0.2799	(0.2656,0.2870)
$Q_{0.975}$	1.9627	(1.6544,2.1554)	1.3462	(0.8420,1.5616)	1.2815	(0.7860,1.5113)	0.3371	(0.3211,0.3524)
$Q_{0.99}$	2.5991	(2.1481,2.9251)	1.8250	(1.1784,2.0496)	1.8240	(1.1285,2.0040)	0.4322	(0.3964,0.4557)

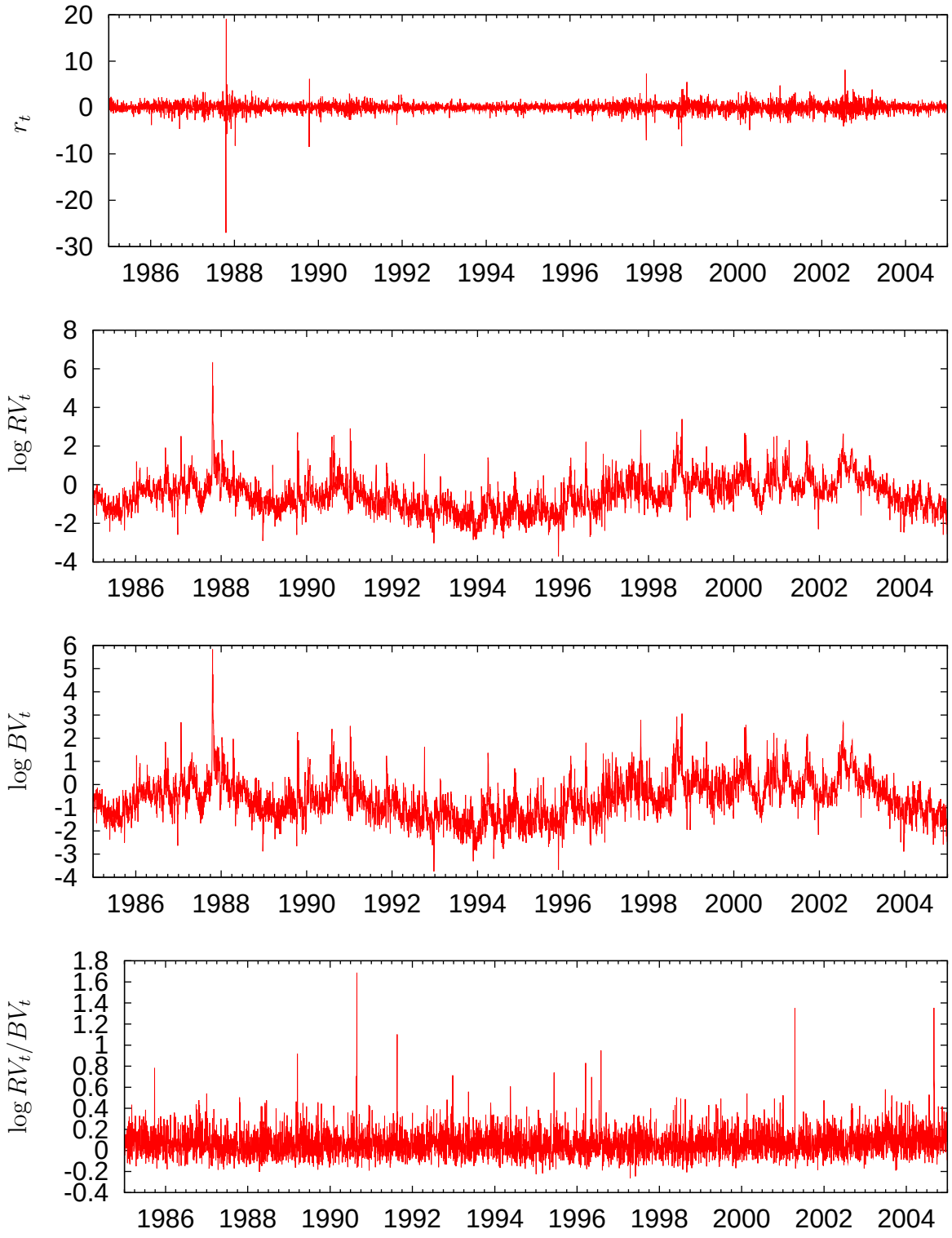

Figure 1: Time Series of returns, logarithmic realized variance, logarithmic Bipower variation and jumps.

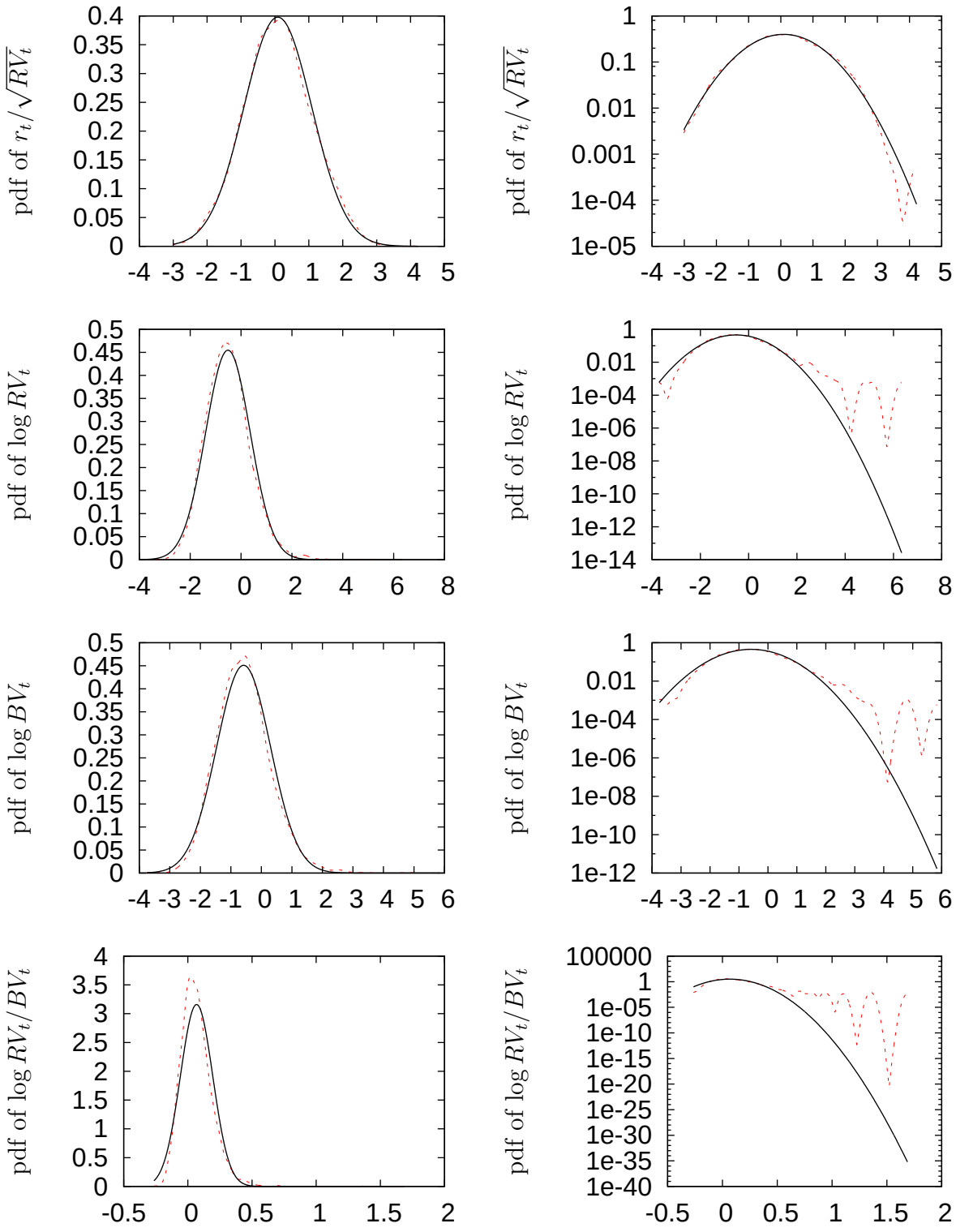

Figure 2: Unconditional distributions of standardized returns, logarithmic realized variance, logarithmic Bipower variation and jumps. The left panel of the figure shows the kernel density estimates of the series (dashed line) and the normal density (solid line) for reference purposes. The right panel shows the same in log scale.

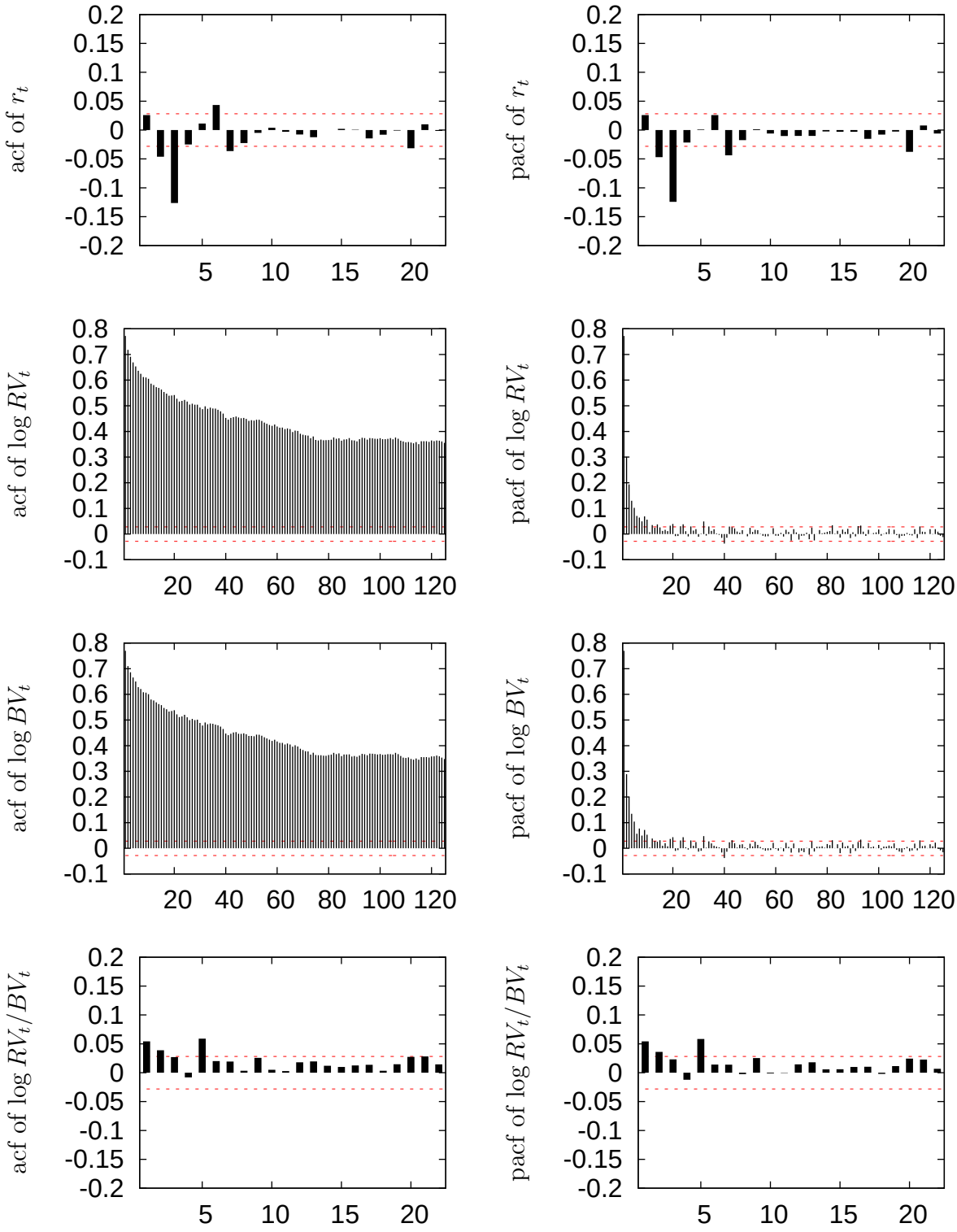

Figure 3: Sample autocorrelations and partial autocorrelations of returns, logarithmic realized variance, logarithmic Bipower variation and jumps. The dashed lines give the upper and lower ranges of the conventional Bartlett 95% confidence band.

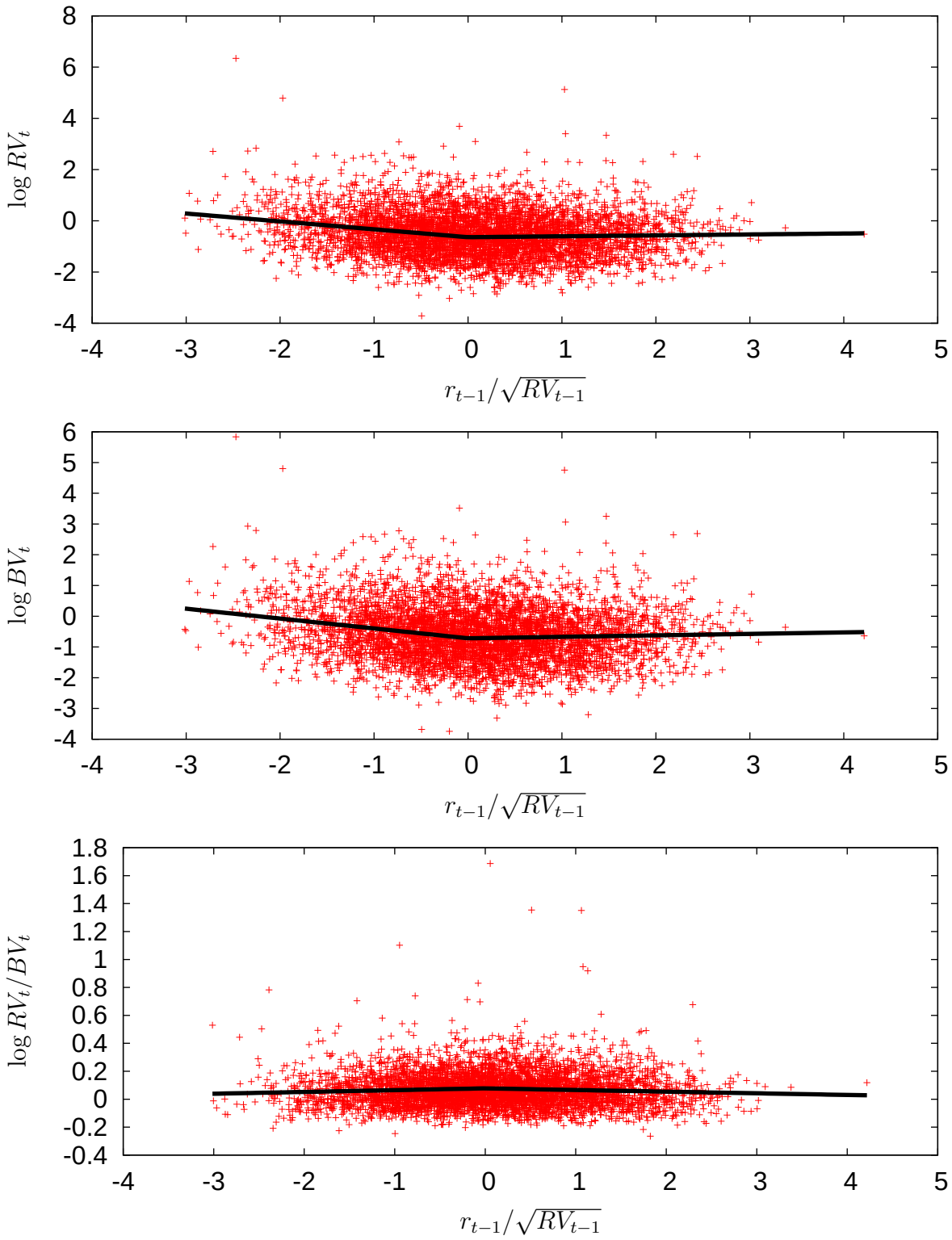

Figure 4: News impact curves for logarithmic realized variance, logarithmic Bipower variation and jumps. The figure shows the scatter points between the respective variable and lagged standardized returns. The solid lines refer the news impact curves, i.e. the linear regression lines for negative and positive values of standardized returns.

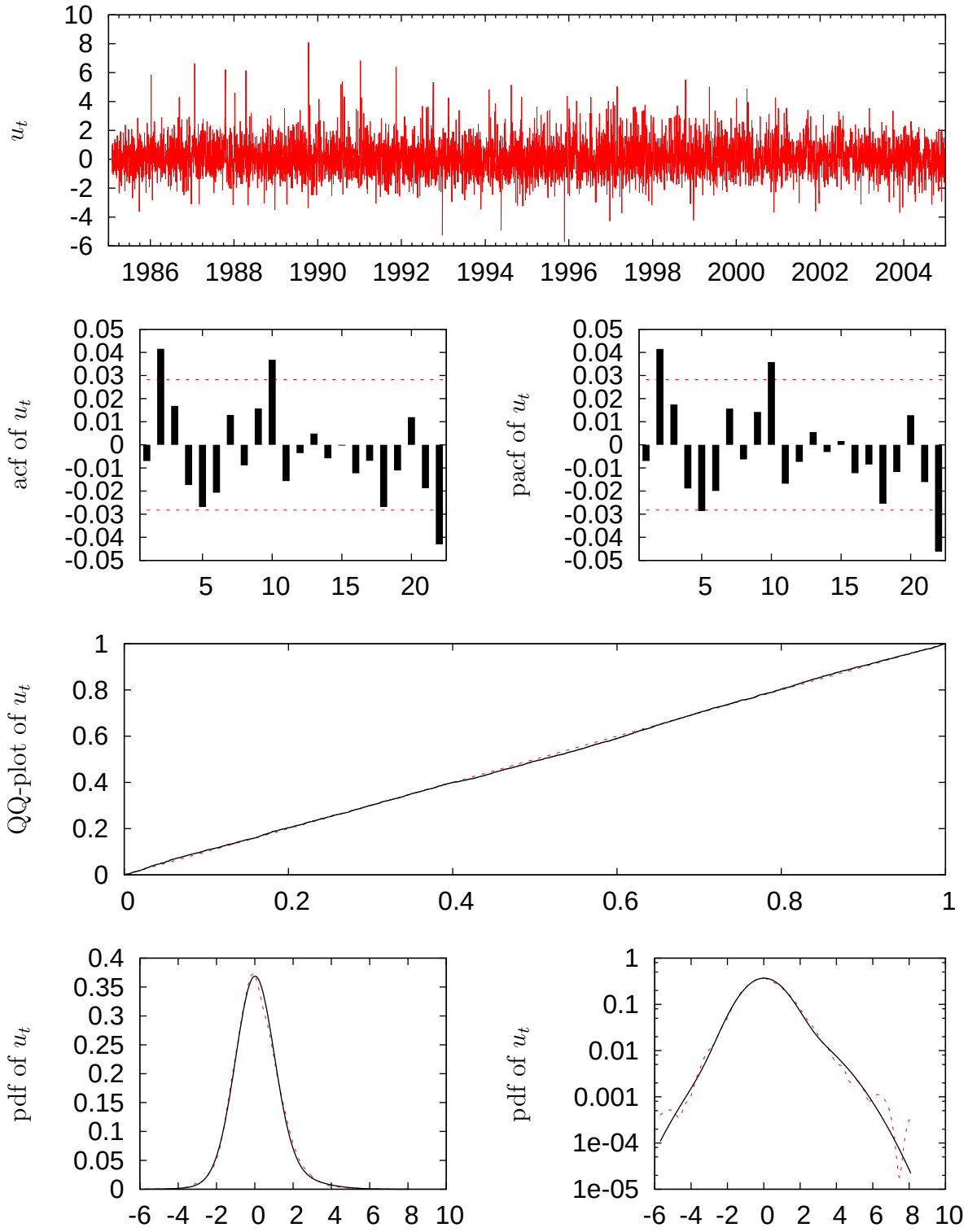

Figure 5: Residual analysis of the (log.) Bipower variation equation. The upper graph of the figure represents the time evolvement of the innovations of the Bipower variation equation. The second line of graphs shows their sample autocorrelations and partial autocorrelations. The third is the corresponding Quantile-Quantile plot. The lower left panel of the figure shows the kernel density estimates of the residuals (dashed line) and the density of the estimated normal mixture (solid line). The right panel shows the same in log scale.

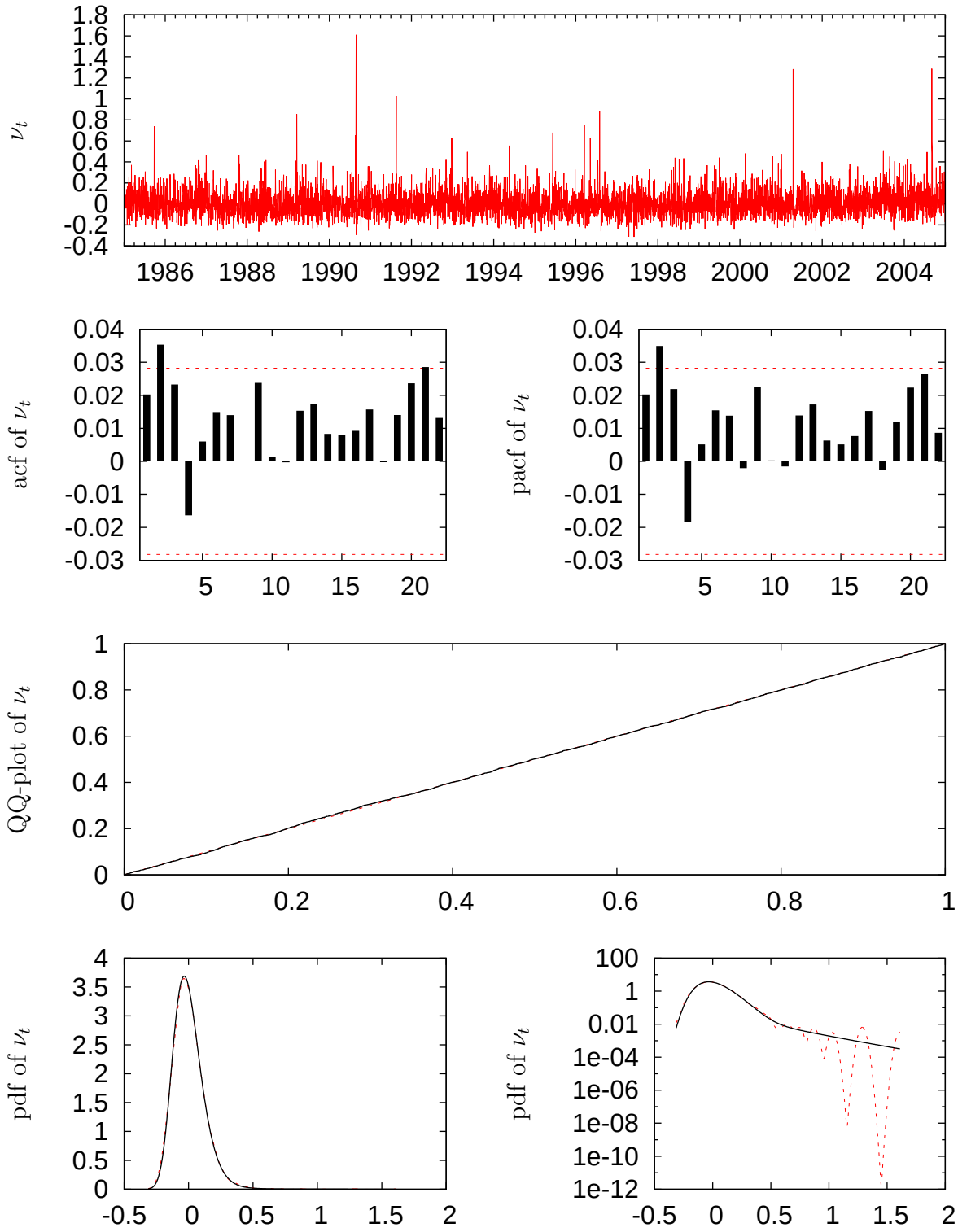

Figure 6: Residual analysis of the jump equation. The upper graph of the figure represents the time evolvement of the innovations of the jump equation. The second line of graphs shows their sample autocorrelations and partial autocorrelations. The third is the corresponding Quantile-Quantile plot. The lower left panel of the figure shows the kernel density estimates of the residuals (dashed line) and the density of the estimated NIG-IG mixture (solid line). The right panel shows the same in log scale.

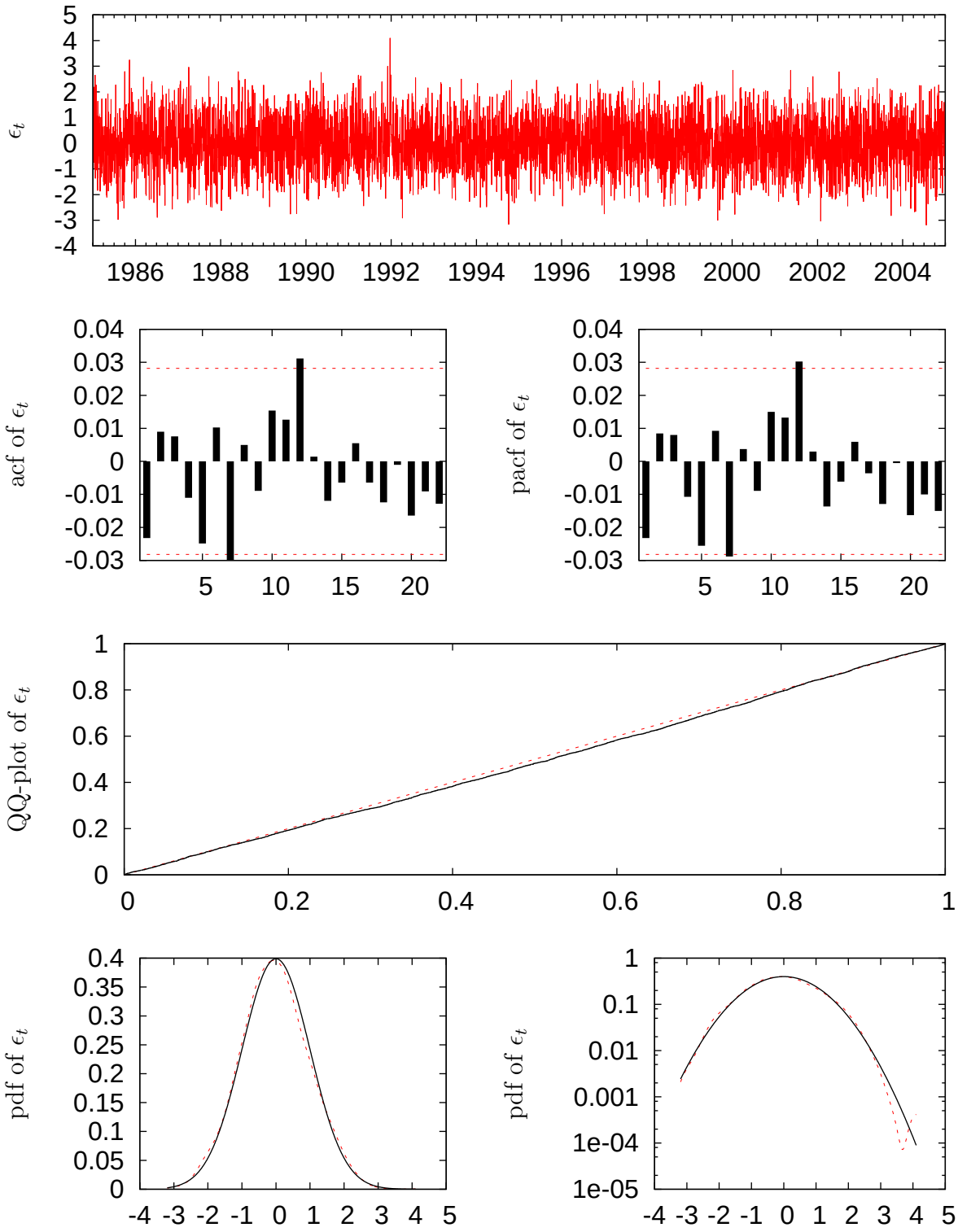

Figure 7: Residual analysis of the return equation. The upper graph of the figure represents the time evolvement of the innovations of the return equation. The second line of graphs shows their sample autocorrelations and partial autocorrelations. The third is the corresponding Quantile-Quantile plot. The lower left panel of the figure shows the kernel density estimates of the residuals (dashed line) and the density of a standard normal (solid line). The right panel shows the same in log scale.

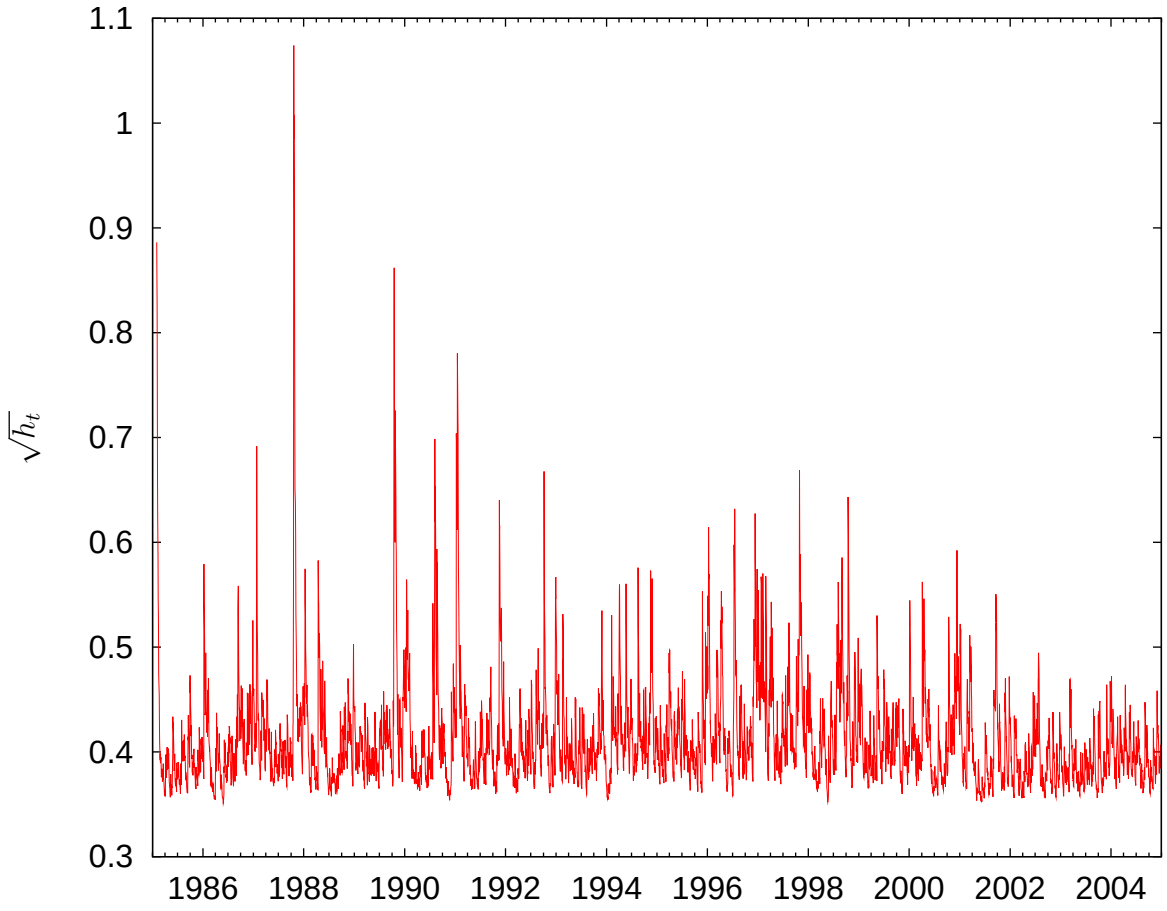

Figure 8: The volatility of Bipower variation. The graph exhibits the HAR-GARCH implied volatility series of logarithmic Bipower variation.

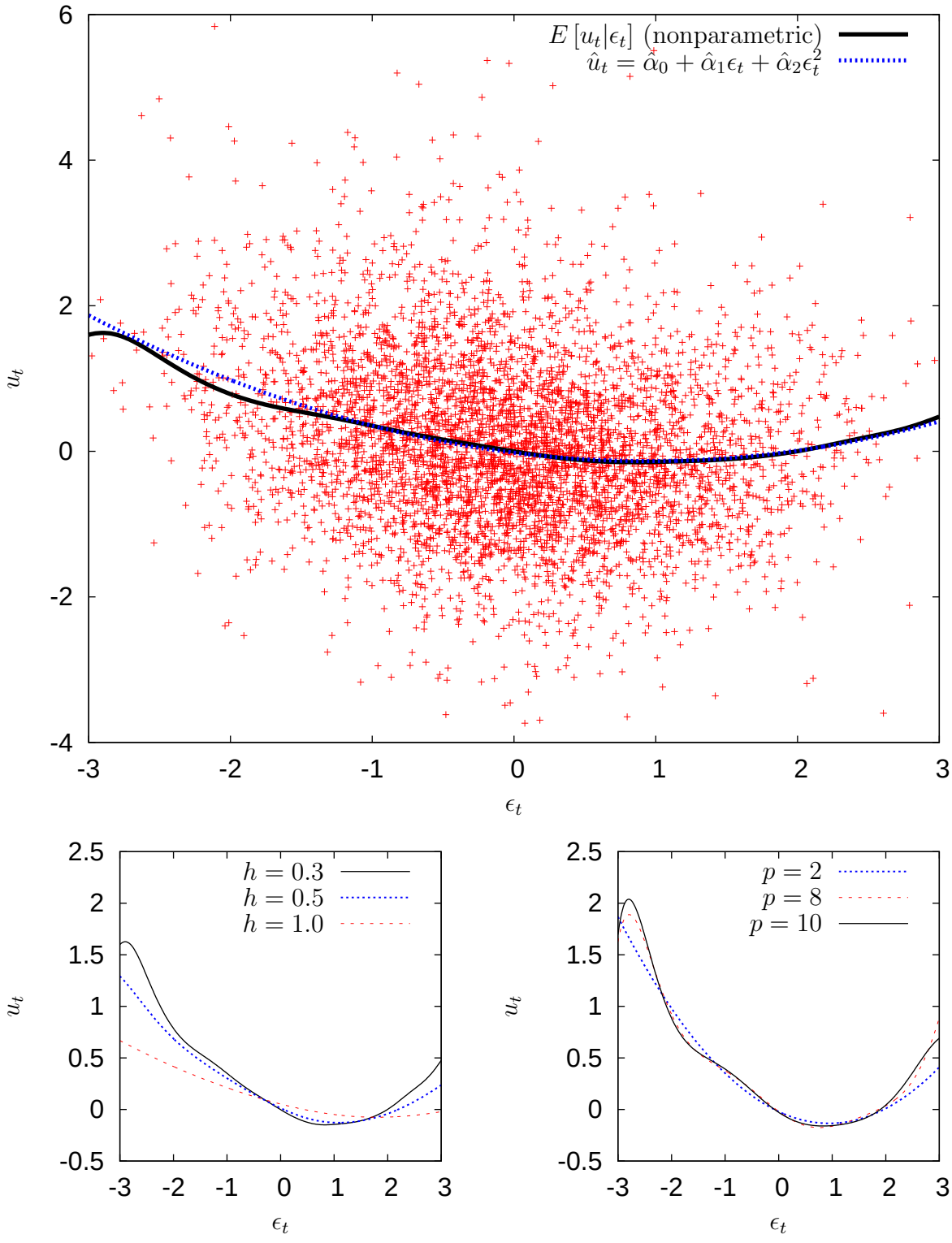

Figure 9: Dependency analysis of the residuals between the return equation and Bipower variation equation. The lower left and right panels include additional different polynomial and nonparametric specifications, respectively.

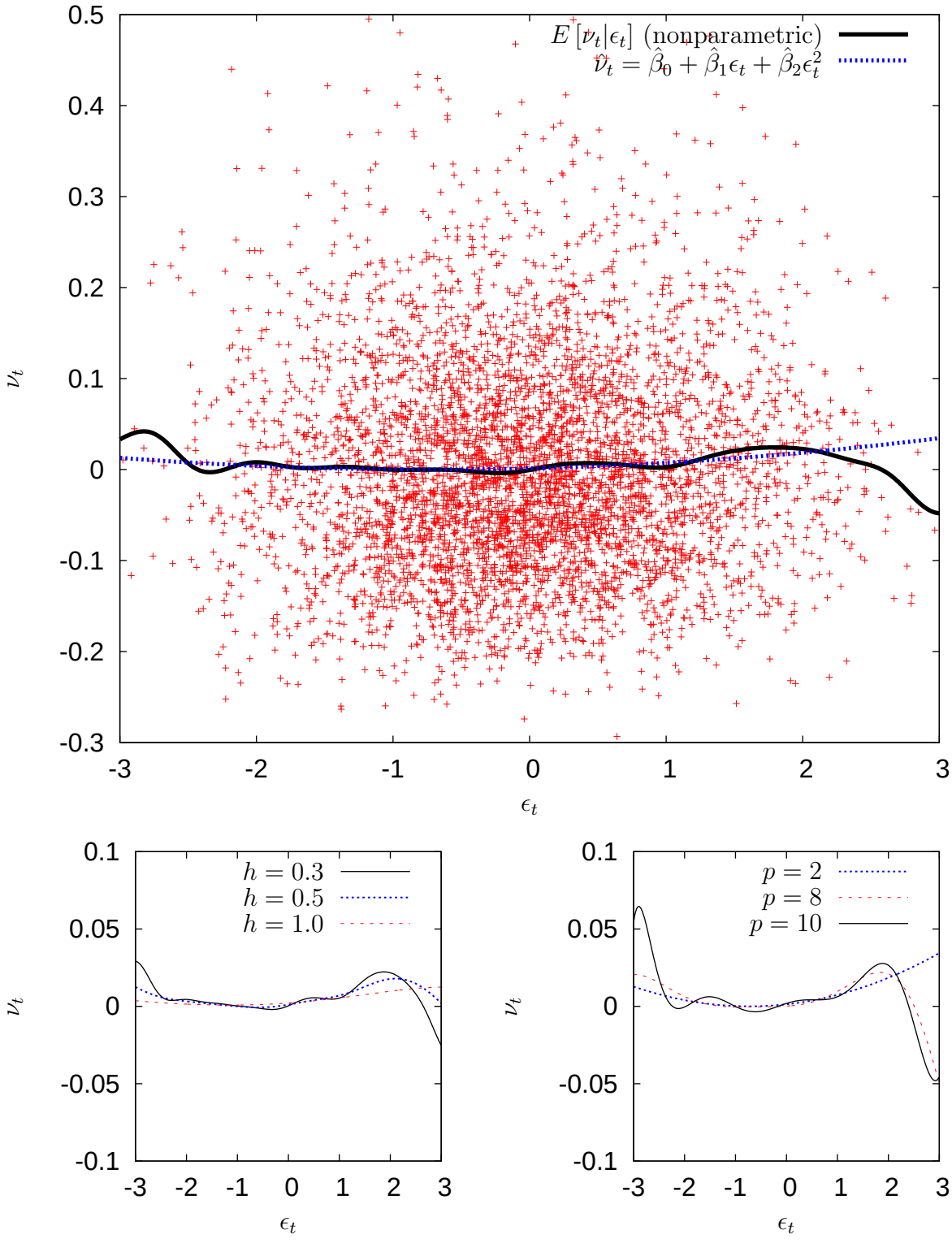

Figure 10: Dependency analysis of the residuals between the return equation and jump equation. The lower left and right panels include additional different polynomial and nonparametric specifications, respectively.

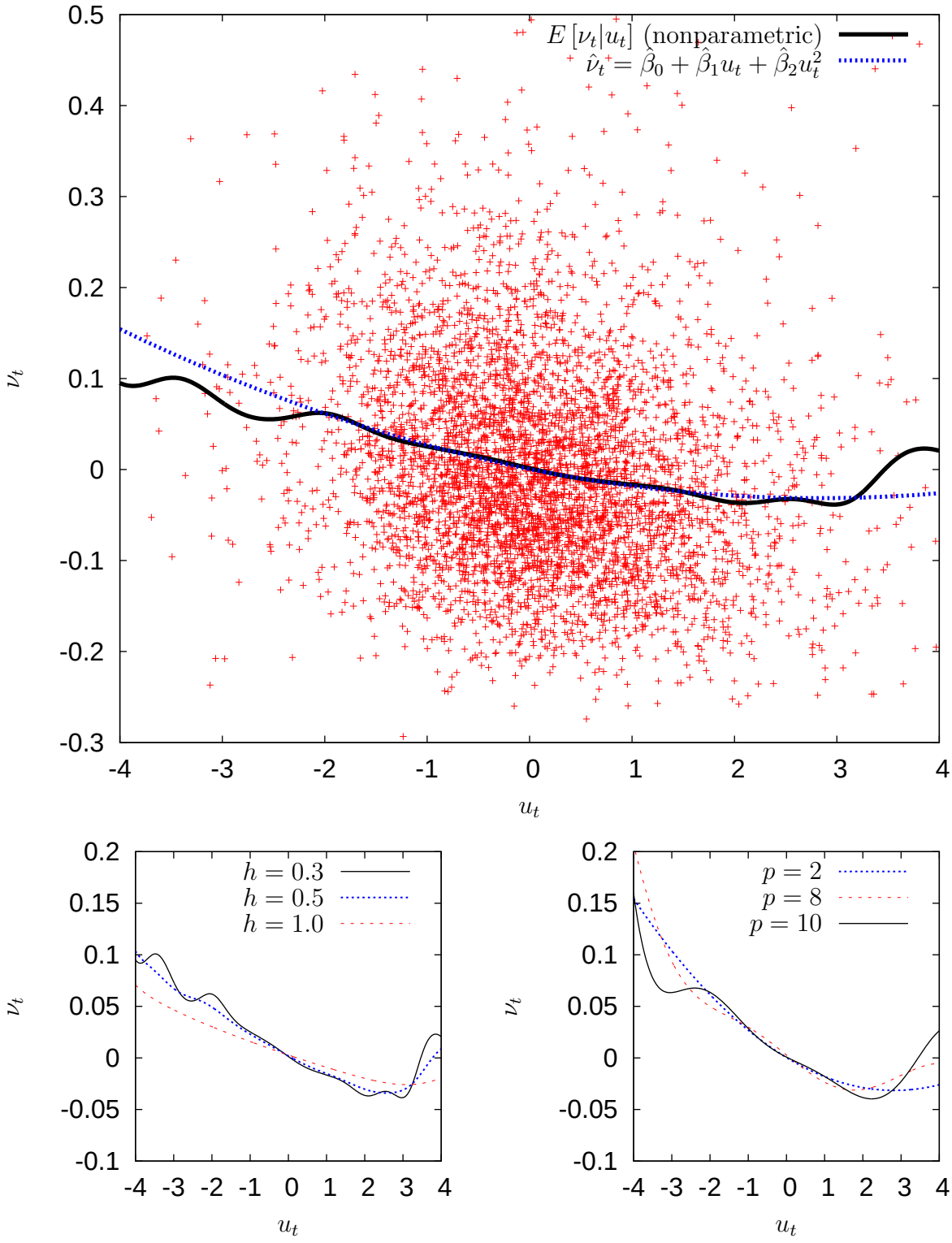

Figure 11: Dependency analysis of the residuals between the Bipower variation equation and the jump equation. The lower left and right panels include additional different polynomial and nonparametric specifications, respectively.

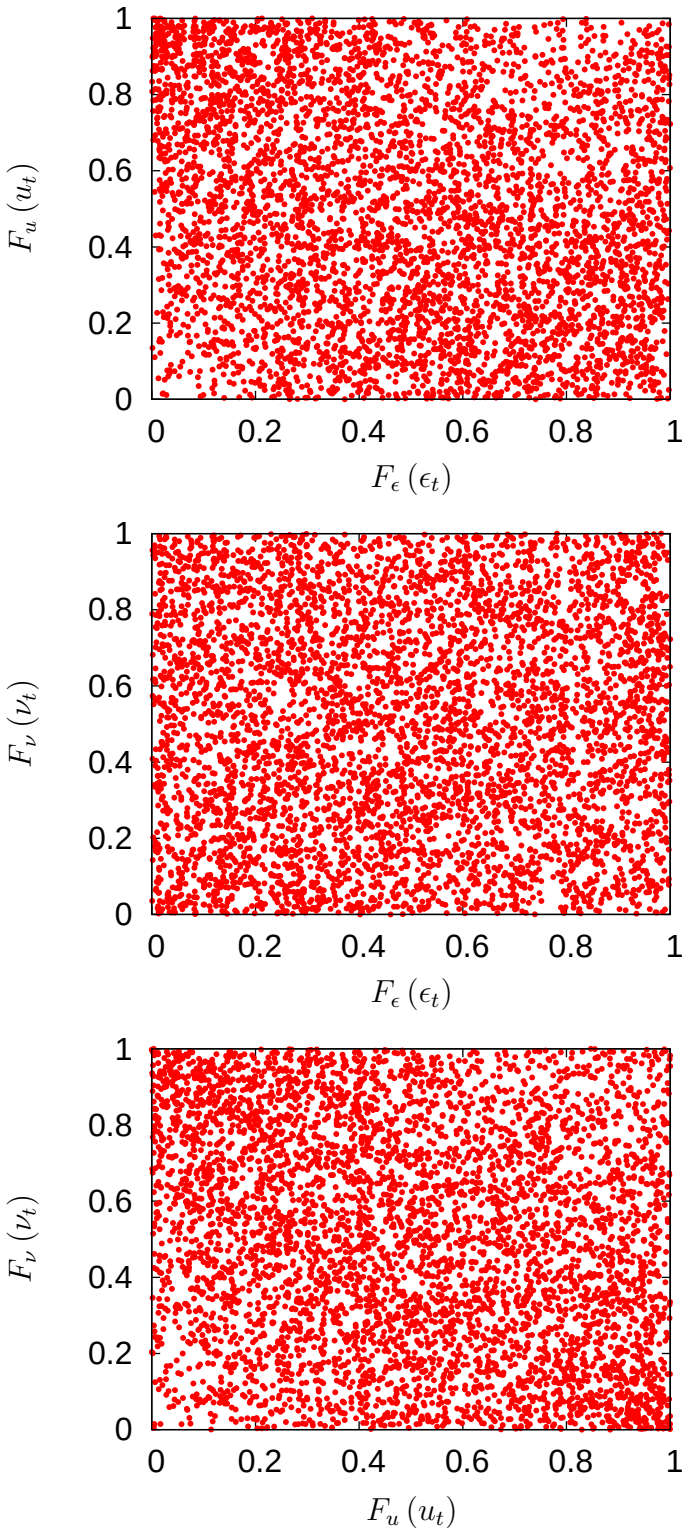

Figure 12: CDF scatter plot of the single equation innovations.

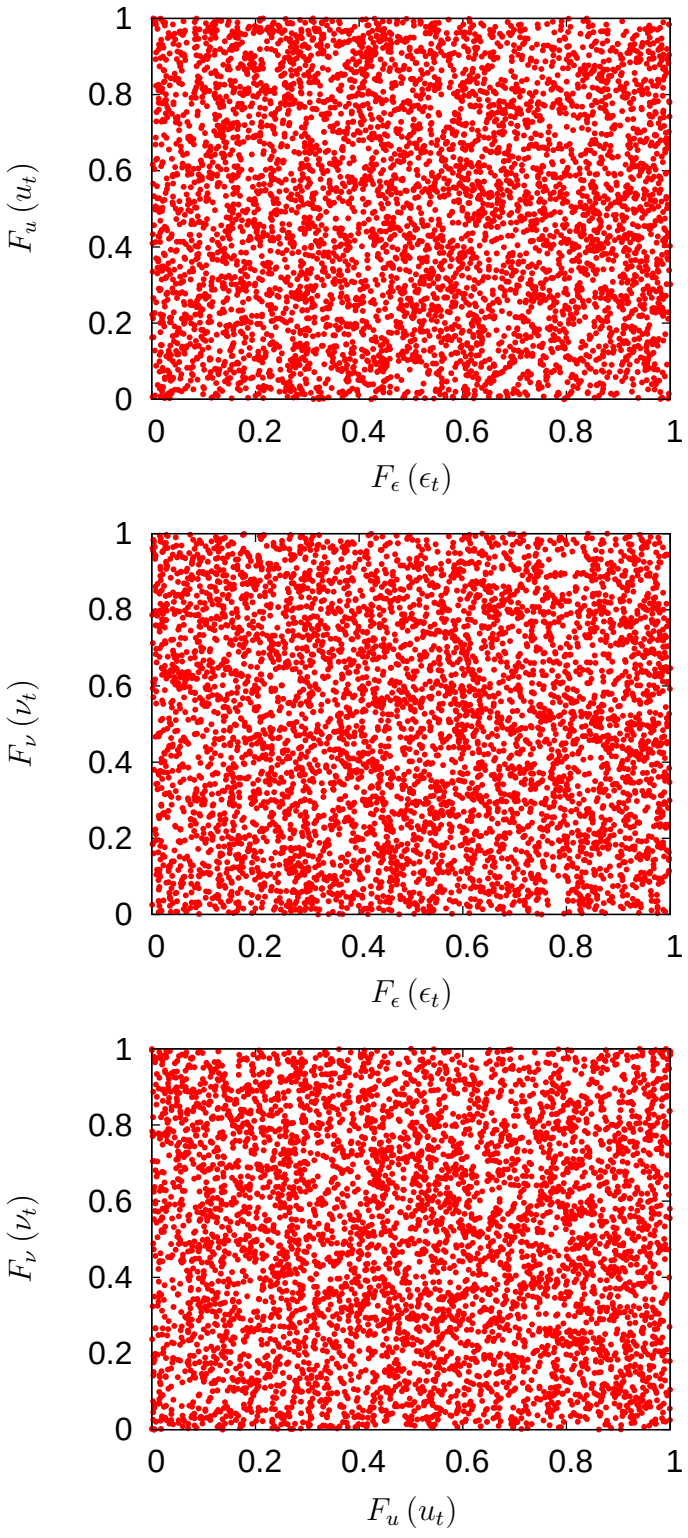

Figure 13: CDF scatter plot of the system innovations.

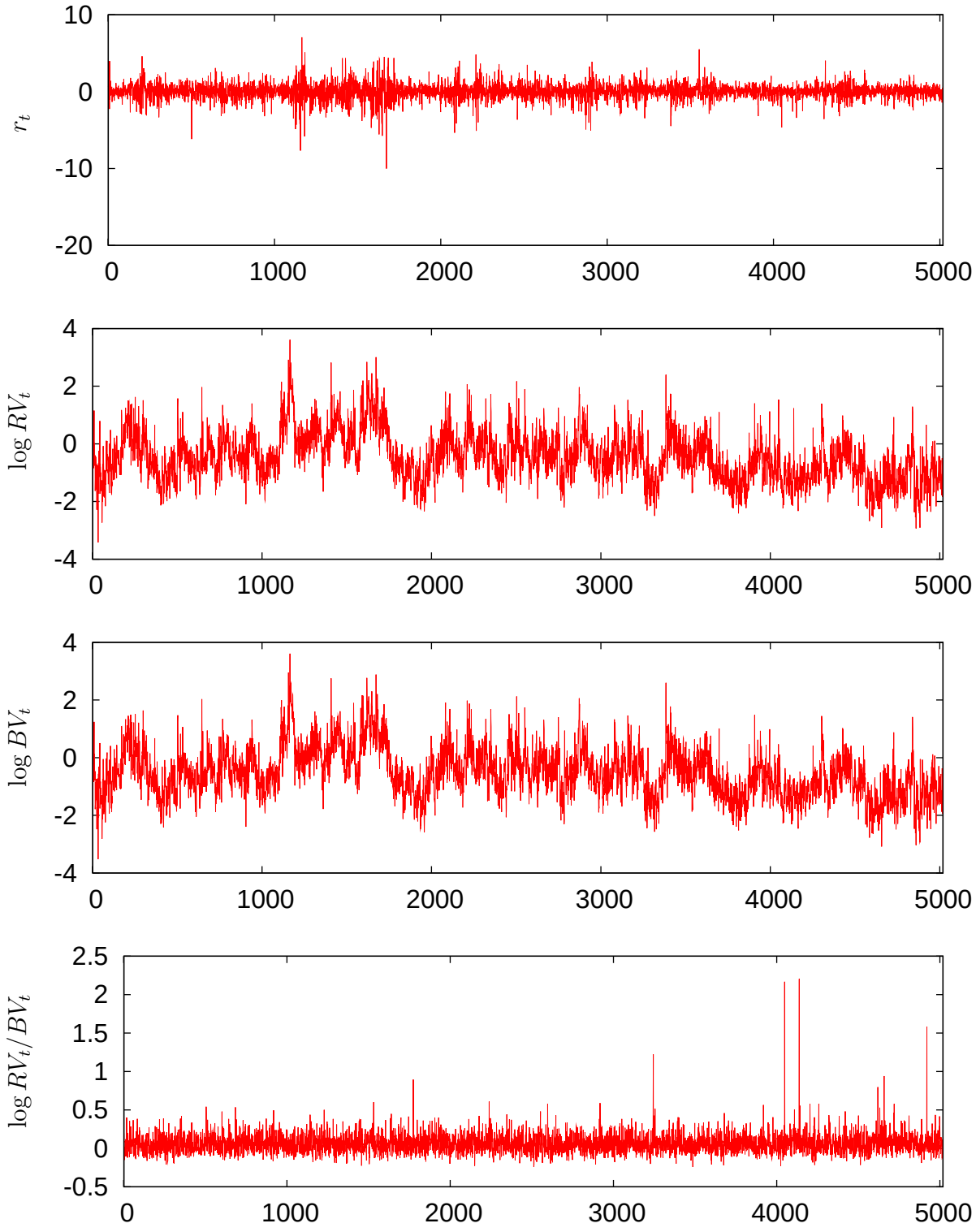

Figure 14: Simulated paths of returns, logarithmic realized variance, logarithmic Bipower variation and jumps.

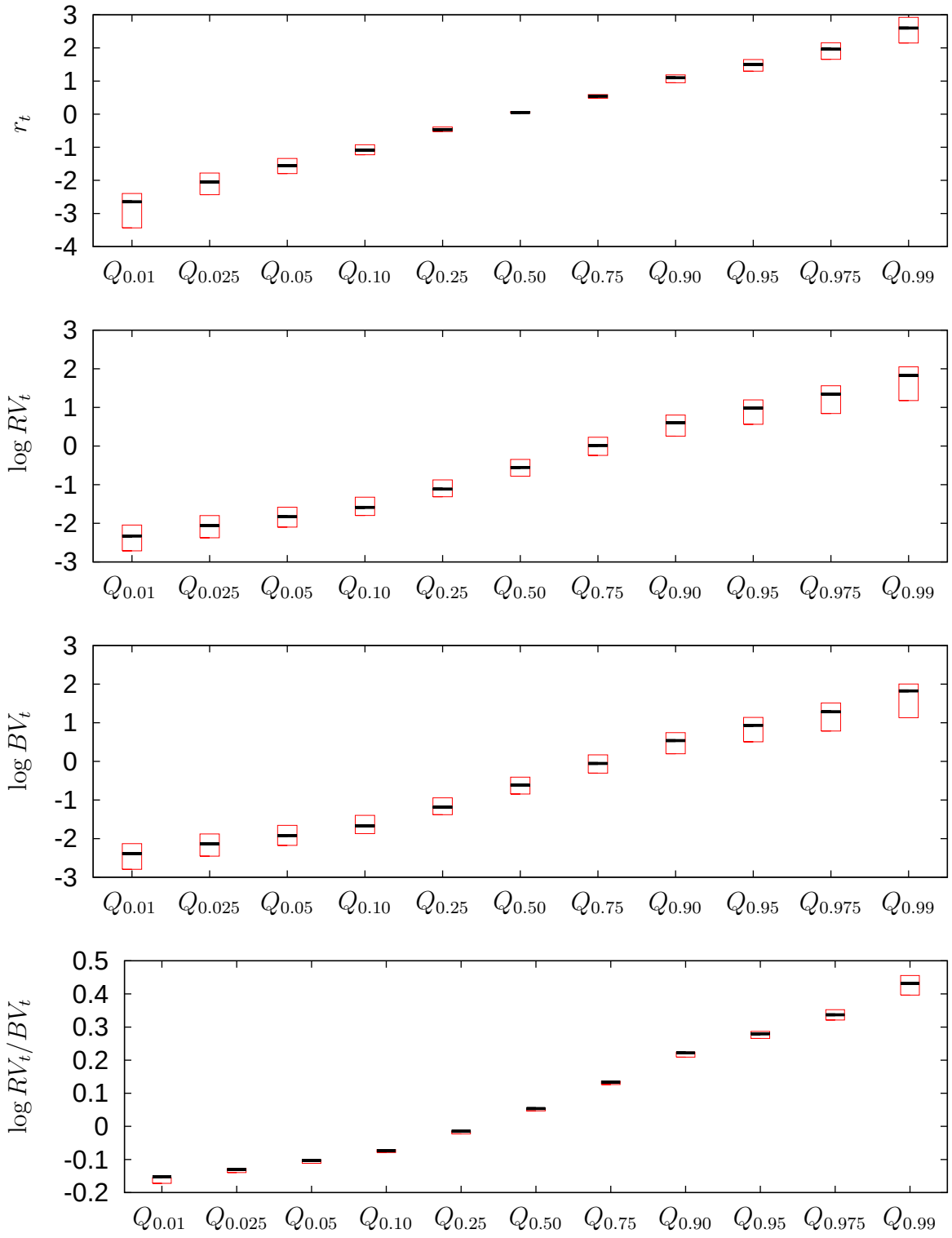

Figure 15: Sample quantiles of returns, logarithmic realized variance, logarithmic Bipower variation and jumps with 95% simulated confidence intervals.

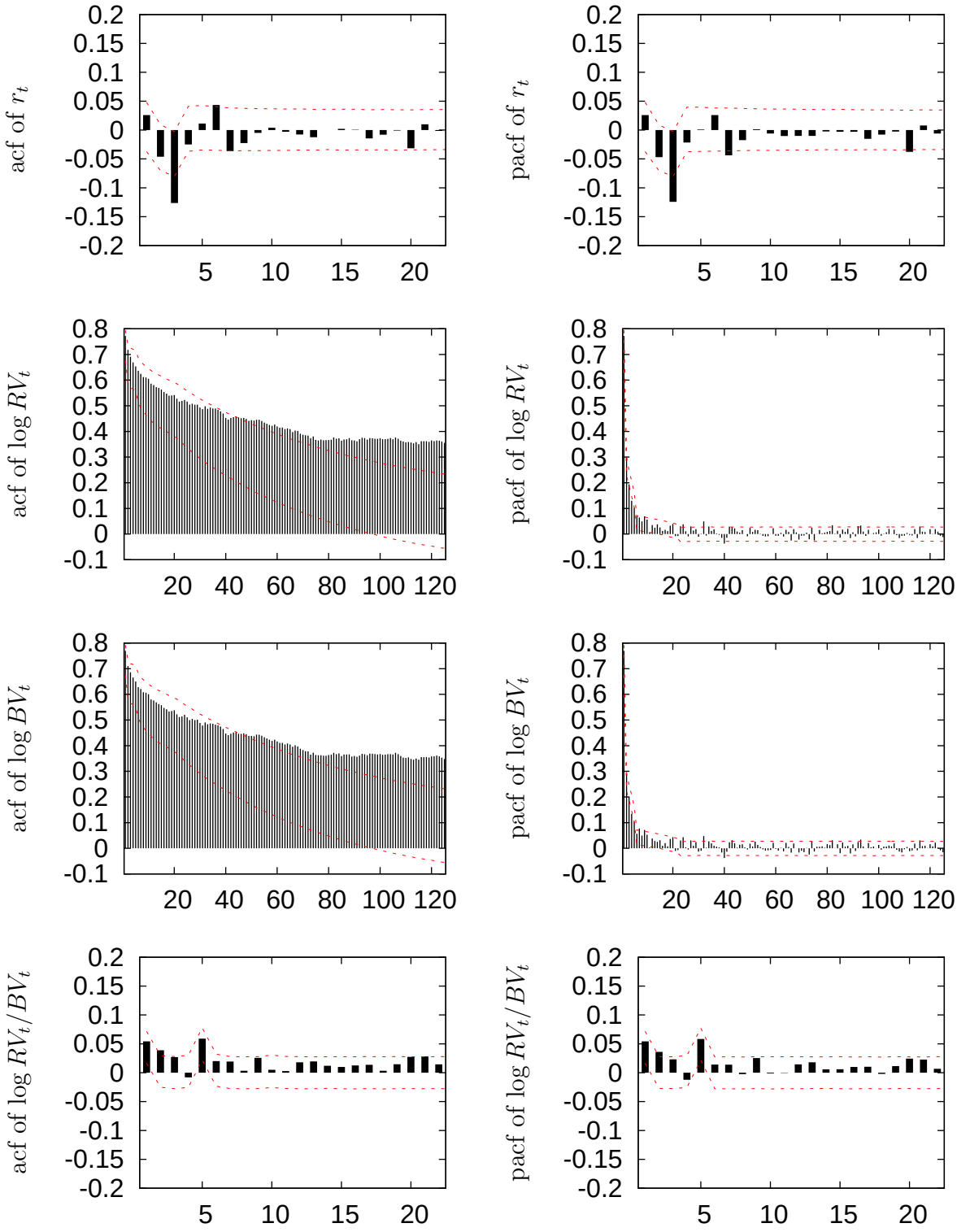

Figure 16: Sample autocorrelations and partial autocorrelations of returns, logarithmic realized variance, logarithmic Bipower variation and jumps. The dashed lines give the upper and lower ranges of the simulated 95% confidence intervals.

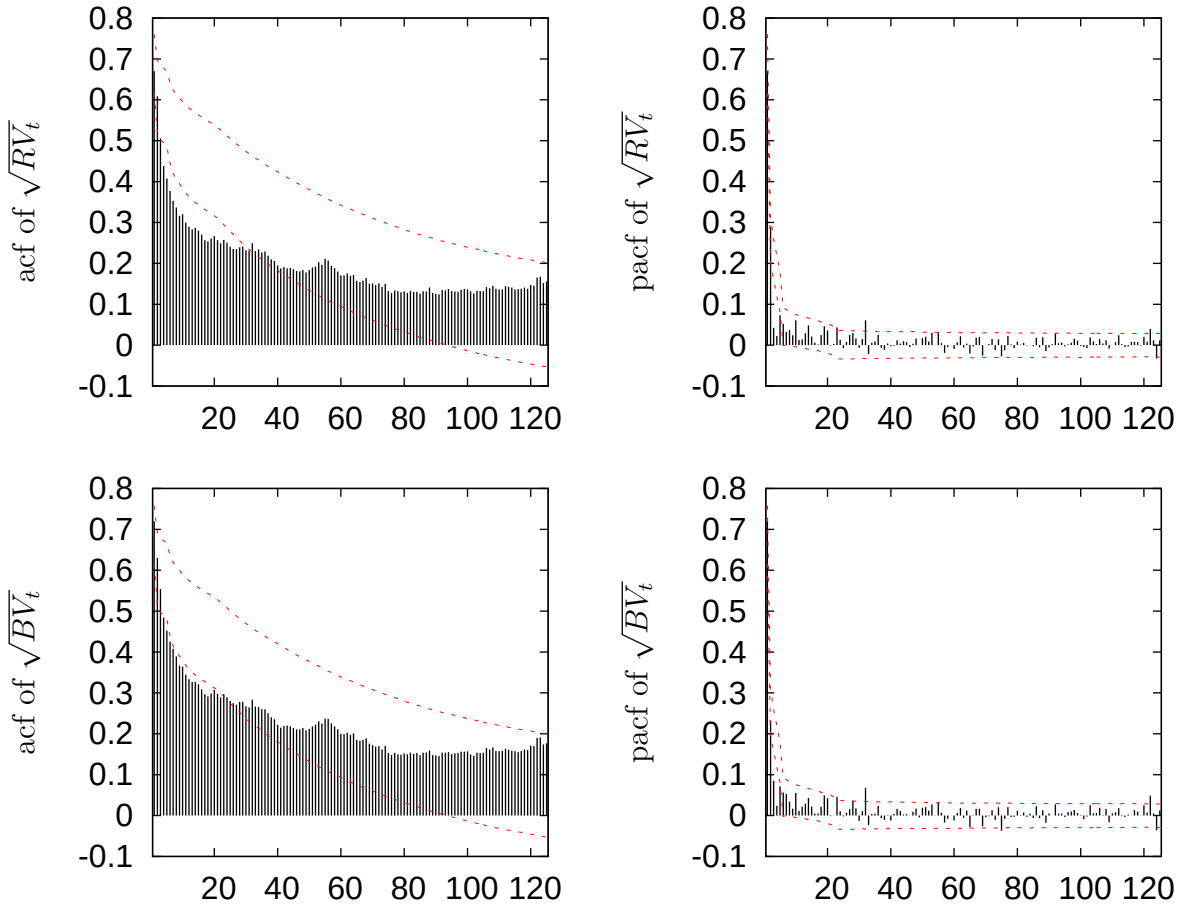

Figure 17: Sample autocorrelations and partial autocorrelations of realized volatility and Bipower variation in standard deviation form. The dashed lines give the upper and lower ranges of the simulated 95% confidence intervals.